

Energy correlations in electron-positron annihilation in quantum chromodynamics: Asymptotically free perturbation theory

C. Louis Basham, Lowell S. Brown, Stephen D. Ellis, and Sherwin T. Love

Department of Physics, University of Washington, Seattle, Washington 98195

(Received 23 October 1978)

In the absence of infrared mass singularities, the asymptotic behavior of cross sections for e^+e^- annihilation in quantum chromodynamics can be expressed entirely in terms of the energy dependence of the renormalization-group running coupling constant. Since the theory is asymptotically free, the running coupling vanishes at high energy, and such infrared-finite cross sections can be calculated perturbatively. We extend previous work by calculating, through second order, the energy-weighted angular correlations of the hadrons produced in e^+e^- annihilation. This involves the computation of quark-antiquark-gluon production and the correction to the lowest-order quark-antiquark production from virtual gluon exchange. A dimensional-continuation scheme is employed to establish that these correlations, taken in a distribution-theory sense, are indeed free of mass singularities. The correlations exhibit interesting features which vanish slowly ($\propto 1/\ln W$) as the energy W increases. We estimate that the nonperturbative, confinement contributions to these features vanish much more rapidly ($\propto 1/W^2$). Thus, effects characteristic of quantum chromodynamics should be quite evident at high energies.

I. INTRODUCTION AND REVIEW

Quantum chromodynamics (QCD),¹ the non-Abelian gauge theory of quarks and gluons, is an extremely attractive candidate for the underlying field theory of hadronic physics. The highly singular infrared nature of the theory and the presence of nontrivial vacuum structure² offer the promise of an explanation for the observed confinement of the basic hadronic constituents but hinder attempts at rigorous calculation. On the other hand, renormalization-group techniques show³ that off-mass-shell amplitudes can be expressed in terms of a running effective coupling $\bar{g}(W)$. The effective coupling in quantum chromodynamics vanishes as the energy W becomes large⁴; it is an asymptotically free theory. A measure of this asymptotic freedom is provided by the parameter $\bar{g}(W)^2/4\pi^2$ which, as will be seen in detail later, controls the QCD contributions to the high-energy total hadronic cross section in electron-positron annihilation.⁵ In the high-energy limit the effective coupling depends upon only one dimensional parameter μ , and we have

$$\frac{\bar{g}(W)^2}{4\pi^2} = \frac{2}{(11 - \frac{2}{3}N_f)\ln(W/\mu)}, \quad (1.1)$$

where N_f is the number of quark types ("flavors"). The parameter μ is taken⁶ to have a value of about 0.5 GeV in order to make the higher-order corrections small. Thus the effective coupling is already quite small at $W=5$ GeV with (assuming $N_f=4$) $\bar{g}(5)^2/4\pi^2=0.10$. This suggests that suitably chosen quantities may be precisely calculated at high energies and the theory of quantum chromo-

dynamics rigorously tested by experiment.

The usual renormalization-group analysis deals with off-mass-shell amplitudes, and contact with experiment is made through an operator-product expansion whose physical matrix elements involve arbitrary functions that describe, roughly speaking, the constituent distributions within hadronic targets. Since these matrix elements are not determined, the theory predicts only the manner in which observables vary with energy but not their magnitudes. Thus, the major experimental tests of QCD, involving deep-inelastic lepton scattering from nuclear targets, are not yet definitive.⁷ The analysis of high-energy electron-positron annihilation, however, avoids such ambiguities since no hadrons appear in the initial state. Recently, Sterman and Weinberg⁸ have suggested that suitably chosen features of the hadronic final states produced in e^+e^- annihilation may be directly calculated by perturbation theory for the production of quarks and gluons, using the small running effective coupling. Of course the experimentally observed final state contains hadrons, not free quarks and gluons. However, as we have discussed previously,⁹ the effects of the transition from the quarks and gluons into the observed hadrons can be treated approximately, using a simple phenomenological model which assumes that limited transverse momenta are produced in these fragmentation processes. The essential result of this treatment, which will be reviewed in some detail below, is that the motion of a produced energetic hadron is closely aligned with that of its parent quark or gluon.

The validity of the use of the running effective

coupling which vanishes at high energies requires that no mass scale appear in this limit other than that provided by the scale parameter μ . Hence, a necessary criterion for a specific feature of the produced hadrons to be "suitably chosen" is that its cross section be finite for massless quarks and gluons. In general, we have no *a priori* rigorous proof that this method of "asymptotically free perturbation theory" is valid. We must resort to perturbation theory to verify that a cross section is indeed free from mass singularities, and this can be done only in low orders.¹⁰ Moreover, we must assume that our fragmentation picture is essentially correct, so that the distributions of quarks and gluons closely approximates those of the observed hadrons. Although the method does lack a completely rigorous foundation, we have no reason to doubt its validity. It does provide precise, unambiguous tests^{8,9,11} of QCD which depend upon no adjustable parameters other than the scale μ . This requires, of course, that the energy is well away from (new-particle) thresholds (e.g. charm threshold).

In general, partial cross sections calculated to some order in perturbation theory will not exhibit a finite limit as the masses of the quarks and gluons vanish; they contain powers of $\ln(W/m)$. These mass singularities will appear if the process is sensitive either to soft-gluon emission or to the collinear branching of a massless quark or gluon into massless quarks and gluons. In particular, the answer to any question referring to a specifically quarklike characteristic (such as the observation of one-third integral charge) will, in general, involve such mass singularities, and it cannot be computed by the method of asymptotically free perturbation theory. One must compute quantities which are "physically sensible"⁸ in the massless limit. The total cross section for e^+e^- annihilation into hadrons is such a "physically sensible" quantity, for it makes no restriction on the nature of the final state. This cross section is the absorptive part of the photon propagator whose high-energy behavior can be evaluated rigorously by renormalization-group techniques. However, at least to second order, the same result is obtained by calculating the processes displayed in Fig. 1, quark-antiquark-gluon production and the virtual-gluon correction to the basic lowest-order quark-antiquark production, using the running effective coupling of Eq. (1) and taking the quarks and gluons to be massless. This is the method of asymptotically free perturbation theory. Note that although the individual graphs of Fig. 1 have infrared mass singularities and must be regulated to be kept finite, the sum which constitutes the total cross section is finite. The result of either

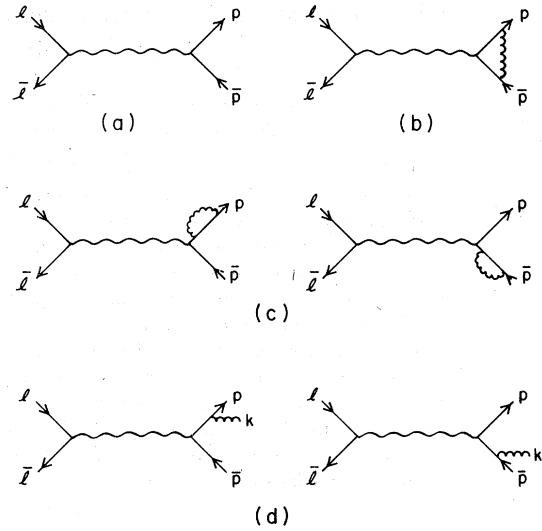


FIG. 1. Zeroth-, first-, and second-order Feynman graphs for electron-positron annihilation. (a) Lowest-order graph for $e^+e^- \rightarrow \gamma \rightarrow q\bar{q}$. (b) Vertex modification. (c) Self-energy insertions. (d) Lowest-order gluon emission graphs.

method is given by

$$\sigma_{\text{tot}} = \frac{4\pi\alpha^2}{3W^2} \sum_f 3Q_f^2 \left[1 + \frac{\bar{g}(W)^2}{4\pi^2} \right], \quad (1.2)$$

where W is the total center-of-mass energy of the e^+e^- collision, $\alpha \approx \frac{1}{137}$ is the fine-structure constant, and Q_f is the fractional charge of a quark of flavor f . (We write Q_f^2 accompanied by the factor 3 to explicitly display the three quark colors which contribute.)

We have proposed⁹ that the total cross section is simply the first member of a hierarchy of increasingly finely grained but still inclusive cross sections which can be calculated by asymptotically free perturbation theory. Each member of this hierarchy entails the detection of the energy carried off by the produced hadrons. This energy weighting should eliminate those singularities associated with soft-gluon emission. Each member also entails the detection of all of the energy passing through some small solid angle with no restriction placed on whether the energy comes from a particular quark or gluon. This inclusive energy summation should eliminate those singularities associated with the collinear branching of massless quarks and gluons. It must be emphasized that the measurement of these energy cross sections does not require any detailed event-by-event analysis as is the case for tests which deal with a quantity involving the definition of a jet axis in each event.^{11(a)} Furthermore, since we consider averaged quantities, they are rather insensitive to experimental fluctuations and the analysis of

the nonperturbative fragmentation corrections is simplified.

[The hierarchy we consider is related to energy correlations involving the stress-energy tensor $T^{\mu\nu}(x)$. Electron-positron annihilation produces a virtual photon which is absorbed by the hadronic electromagnetic current $j^\mu(z)$. The total cross section is related to the vacuum expectation value of two current operators $\langle j^\mu(z)j^\nu(z') \rangle_0$. The subsequent members of the hierarchy correspond to the vacuum matrix elements $\langle j^\mu(z)T^{00}(x_1)j^\nu(z') \rangle_0$, $\langle j^\mu(z)T^{00}(x_1)T^{00}(x_2)j^\nu(z') \rangle_0$, and so forth. Here the spacetime coordinates x_1^μ, x_2^μ, \dots of the detectors are far removed from the annihilation region described by the coordinates z, z' of the current operators. Therefore the usual technique of the renormalization group with its short-distance operator-product expansion is not applicable, and the perturbation theory we have described must be used instead.]

In our previous paper,⁹ we have discussed the differential energy cross section $d\Sigma/d\Omega$ which is the simplest partial cross section of the hierarchy. It describes the angular "antenna" pattern of the hadronic energy produced by e^+e^- collisions. The energy cross section could be determined, for example, by measurements with a small hadronic calorimeter placed at various angular positions. If the calorimeter collects an energy ΔE in a solid angle $d\Omega$ during a time ΔT , then $d\Sigma/d\Omega = \Delta E / (W\mathcal{L}\Delta T d\Omega)$, where \mathcal{L} is the luminosity of the e^+e^- colliding beams. We note that this determination is in accord with the general characteristic emphasized previously: It does not require detailed measurements on each of the particles produced in a single event. Since the energy cross section involves simply the detection of the energy passing through some small solid angle, without regard to the specific hadrons which carry this energy, it is insensitive to both soft-gluon emission and to the collinear branching of the massless quarks and gluons, and it should be calculable with the method of asymptotically free perturbation theory. The absence of mass singularities is borne out by explicit calculations in second order⁹ which involve the graphs displayed in Fig. 1. Although the individual graphs do have mass singularities, these singularities cancel in the construction of the energy cross section. For the sake of clarity we shall review our previous results⁹ and refine them by considering the corrections resulting from heavy-lepton production.

The energy pattern cross section can be expressed in terms of partial cross sections

$$\frac{d^N\sigma}{E_1^{-1}(d^3p_1) \cdots E_N^{-1}(d^3p_N)}$$

for the process $e^+e^- \rightarrow N$ hadrons at total energy W . The general form is given by

$$\frac{d\Sigma}{d\Omega} = \sum_{N=2}^{\infty} \int \prod_{a=1}^N E_a^{-1}(d^3p_a) \frac{d^N\sigma}{E_1^{-1}(d^3p_1) \cdots E_N^{-1}(d^3p_N)} \times S_N \sum_{b=1}^N \frac{E_b}{W} \delta(\Omega - \Omega_b), \quad (1.3)$$

where S_N represents the statistical weights necessary to avoid multiple counting of identical particles. Integrating this general form over all solid angle produces a factor $\sum_{b=1}^N E_b/W$ which, by energy conservation, is unity, and thus we have the normalization

$$\int d\Omega \frac{d\Sigma}{d\Omega} = \sigma_{\text{tot}}, \quad (1.4)$$

where σ_{tot} is the total hadronic cross section. The observed N -particle final state involves, of course, N hadrons. In our perturbative method, the N hadrons are replaced by massless quarks, antiquarks, and massless gluons. We shall describe the effects of the fragmentation process connecting the quarks and gluons with the observed hadrons in some detail in subsequent paragraphs. The production cross sections for massless quarks and gluons are divergent. However, as indicated above, these singularities cancel in the sum defining the energy cross section.

Electron-positron annihilation at high energy produces a virtual photon with a spin density matrix given by

$$L_{jk} = \frac{1}{2}(1 - P^2)(\delta_{jk} - \hat{l}_j \hat{l}_k) + P^2 \hat{b}_j \hat{b}_k. \quad (1.5)$$

Here \hat{l} and \hat{b} denote the directions of the beam and the magnetic field, respectively, which are orthogonal ($\hat{l} \cdot \hat{b} = 0$), and P ($-P$) is the polarization of the electron (positron) along the magnetic field direction. Clearly, the unpolarized form ($P = 0$) is obtained from the perfectly polarized form ($P = 1$) by averaging \hat{b} over two directions perpendicular to \hat{l} . But the perfectly polarized form can also be obtained from the unpolarized form. For example, the identity

$$\hat{z}_j \hat{z}_k = \frac{1}{2}(\delta_{jk} - \hat{x}_j \hat{x}_k) + \frac{1}{2}(\delta_{jk} - \hat{y}_j \hat{y}_k) - \frac{1}{2}(\delta_{jk} - \hat{z}_j \hat{z}_k)$$

expresses the density matrix for perfect polarization along the z axis in terms of the unpolarized density matrix for beams along the x , y , and z axes. Therefore, in principle, experiments with polarized beams yield no new information since a rotation of the beam axis is equivalent to a rotation of the detection apparatus. However, in practice, experimental accuracy may be significantly improved by using partially polarized beams while theoretical calculations are most simply performed for perfect polarizations. Hence we calculate for

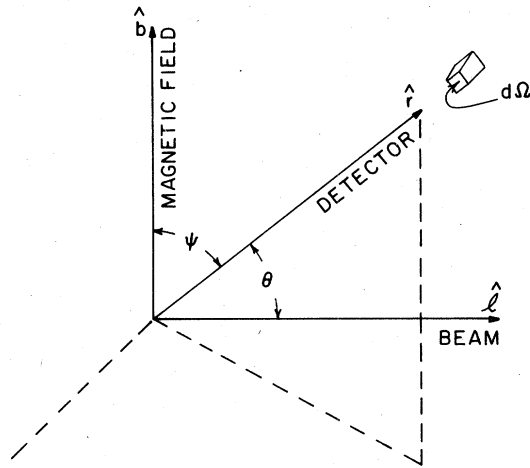


FIG. 2. Geometry for the energy-pattern experiment.

perfect polarization but, using trivial substitutions, present our results for arbitrary polarization.

The energy cross section in lowest order arises

$$\frac{d\Sigma^{(\text{QCD})}}{d\Omega} = \frac{\alpha^2}{2W^2} \sum_f 3Q_f^2 \left\{ \left(1 + \frac{\bar{g}(W)^2}{4\pi^2} \right) [P^2 \sin^2 \psi + \frac{1}{2}(1-P^2)(1+\cos^2 \theta)] + \frac{\bar{g}(W)^2}{4\pi^2} [P^2(3\cos^2 \psi - 1) + \frac{1}{2}(1-P^2)(1-3\cos^2 \theta)] \right\}, \quad (1.7)$$

with the effective coupling $\bar{g}(W)^2/4\pi^2$ given by Eq. (1.1). This angular distribution is most easily described for the case of perfect polarization ($P=1$). In the high-energy limit it is a $\sin^2 \psi$ distribution which vanishes along the magnetic field direction. As the energy is lowered, the dips are filled in by the $\bar{g}(W)^2$ correction as shown in Fig. 3(a). The angular distribution for the unpolarized case is illustrated in Fig. 3(b).

Perturbative QCD results must be corrected for the fragmentation of the quarks and gluons into the observed hadrons. A precise calculation of these corrections is clearly a very difficult task, for it involves the details of the confinement mechanism. We will obtain a rough estimate of the size of these corrections by using a simple phenomenological model. Although this estimate will be a rough approximation, it will give a good indication of the size of the nonperturbative "background" which the perturbative QCD modifications must exceed if they are to be measurable. Since the fragmentation effects will be small, we may view them simply as a correction to the lowest-order quark-antiquark process [Fig. 1(a)]. We assume that the high-energy quark or antiquark produces a "jet" of hadrons whose transverse momenta are limited, with the number of hadrons in the jet

from the quark-antiquark production depicted in Fig. 1(a), and it is identical with the ordinary differential cross section,

$$\begin{aligned} \frac{d\Sigma^{(0)}}{d\Omega} &= \frac{d\sigma}{d\Omega} \\ &= \frac{\alpha^2}{2W^2} \sum_f 3Q_f^2 [P^2 \sin^2 \psi + \frac{1}{2}(1-P^2)(1+\cos^2 \theta)]. \end{aligned} \quad (1.6)$$

The definition of the angles θ and ψ is illustrated in Fig. 2. They are the polar angles of the detection direction \hat{r} with respect to the beam axis \hat{l} and the magnetic-field orientation \hat{b} , $\cos \theta = \hat{r} \cdot \hat{l}$, $\cos \psi = \hat{r} \cdot \hat{b}$. The result (1.6) is the infinite-energy limit where the effective coupling $\bar{g}(W)$ vanishes. The perturbative corrections must be evaluated for finite energies. In second order, these corrections involve the virtual-gluon exchange shown in Figs. 1(b) and 1(c) and the real-gluon emission shown in Fig. 1(d). To this order we have

growing logarithmically with the total energy of the jet, $\langle n \rangle_{\text{jet}} \sim \frac{1}{2} C \ln(W/2)$. More precisely, we assume that a quark (or antiquark) fragments into a number dn of hadrons in a momentum interval (d^3h) given by the scaling distribution

$$dn = \frac{(d^3h)}{h^0} f(z, h_{\perp}), \quad (1.8)$$

where $z = 2h_{\parallel}/W$, with h_{\parallel} and h_{\perp} the components of the emitted hadron momentum \vec{h} which are parallel and perpendicular to the quark (or antiquark) direction, respectively. Then, as shown in our previous work,⁹ which is reviewed and extended in Appendix B, the fragmentation correction to the lowest-order energy cross section (1.6) gives [cf. Eq. (B19)]

$$\begin{aligned} \frac{d\Sigma^{(\text{qt})}}{d\Omega} &= \frac{\alpha^2}{2W^2} \sum_f 3Q_f^2 \{ [P^2 \sin^2 \psi + \frac{1}{2}(1-P^2)(1+\cos^2 \theta)] \\ &\quad + \frac{1}{2} \langle \sin^2 \eta \rangle^{(\text{qt})} [P^2(3\cos^2 \psi - 1) \\ &\quad + \frac{1}{2}(1-P^2)(1-3\cos^2 \theta)] \}. \end{aligned} \quad (1.9)$$

Here η is a "jet opening angle", the angle that the emitted hadron makes with the direction of its quark (or antiquark) parent, and $\langle \sin^2 \eta \rangle^{(\text{qt})}$ is the

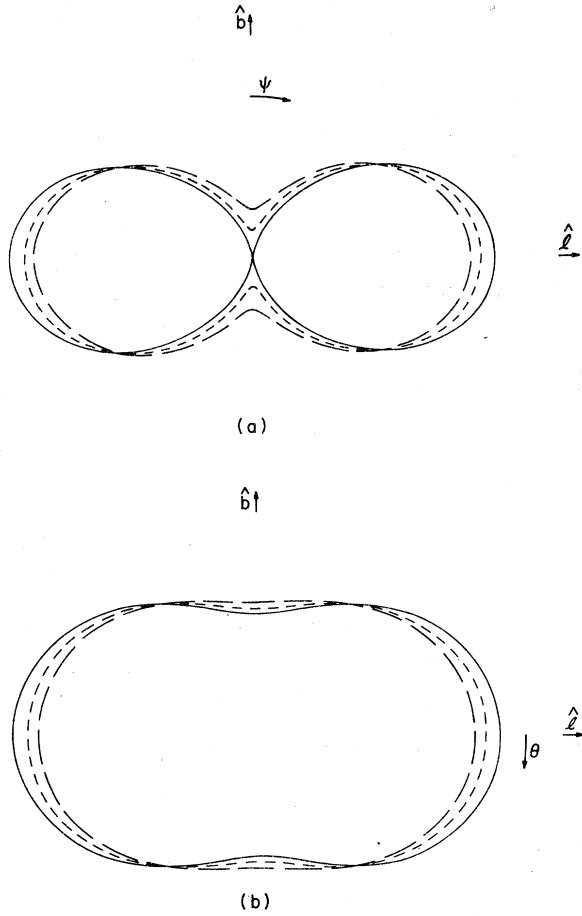


FIG. 3. (a) QCD predictions for the normalized antenna patterns $(1/\sigma_{\text{tot}})(d\Sigma/d\Omega)$ corresponding to perfectly polarized electron and positron beams with various total energies W . The long dashed curve corresponds to $W = 5$ GeV, the short dashes to $W = 30$ GeV, and the solid curve is for infinite W . All unit vectors and angles refer to the geometry displayed in Fig. 2. (b) Same as (a) except that the electron-positron beams are unpolarized.

energy-weighted average with the distribution (1.8). In the high-energy limit

$$\langle \sin^2 \eta \rangle^{(\text{qt})} \simeq \frac{\pi C \langle h_{\perp} \rangle}{2W}, \quad (1.10)$$

where $\langle h_{\perp} \rangle$ is the average transverse momentum

of an emitted hadron and C is the coefficient of the logarithmic increase in the total multiplicity of the hadrons produced in e^+e^- collisions,

$$\langle n \rangle_{\text{tot}} \simeq C \ln W + \text{const.} \quad (1.11)$$

We see that the fragmentation process also smears the energy pattern, filling in its minima. However, this correction vanishes as $1/W$ as the energy increases. It vanishes much more rapidly than does the perturbative QCD effect which behaves as $1/\ln W$. Figure 4 displays the size of the fragmentation correction for the parameters¹² $C = 2.5$ and $\langle h_{\perp} \rangle = 0.3$ GeV. Note that the perturbative QCD energy pattern (1.7) and the fragmentation pattern (1.9) have identical structure. Comparing the two results, we get an identification of a "jet opening angle" for the perturbative QCD contribution:

$$\langle \sin^2 \eta \rangle^{(\text{QCD})} \simeq 2 \frac{\bar{g}(W)^2}{4\pi^2} = \frac{4}{(11 - \frac{2}{3}N_f) \ln(W/\mu)}. \quad (1.12)$$

The semihadronic decays of heavy leptons into neutrinos and hadrons gives further corrections. In practice, these processes cannot be separated from the purely hadronic events. However, they give rise to very small effects so that a crude approximation suffices for their description. As explained in detail in Appendix B, we assume that the heavy lepton produces an isotropic distribution of hadrons in its rest frame. With this hypothesis, the hadronic energy pattern resulting from heavy-lepton decays can be computed without the introduction of any new parameter [cf. Eqs. (B22)–(B32)]. In the high-energy limit the result is identical with the quark-fragmentation expression (1.9) except for two alterations. The quark-charge factor $\sum_f 3Q_f^2$ is replaced by $\beta^2 \gamma$, where β is the branching ratio for a single heavy lepton to decay into hadrons, and γ is the average fraction of the heavy-lepton energy carried off by detectable hadrons with the remaining fraction $(1 - \gamma)$ escaping in undetected neutrinos. The jet-opening-angle factor $\langle \sin^2 \eta \rangle^{(\text{qt})}$ is replaced by $8M^2/W^2$ where M is the mass of the heavy lepton. Thus, summing all corrections, the energy pattern cross section in leading order reads

$$\frac{d\Sigma}{d\Omega} = \frac{\alpha^2}{2W^2} \left\{ \left[\left(1 + \frac{\bar{g}(W)^2}{4\pi^2} \right) \sum_f 3Q_f^2 + \beta^2 \gamma \right] [P^2 \sin^2 \psi + \frac{1}{2}(1 - P^2)(1 + \cos^2 \theta)] \right. \\ \left. + \left[\left(\frac{\bar{g}(W)^2}{4\pi^2} + \frac{1}{2} \langle \sin^2 \eta \rangle^{(\text{qt})} \right) \sum_f 3Q_f^2 + \frac{4M^2}{W^2} \beta^2 \gamma \right] [P^2(3 \cos^2 \psi - 1) + \frac{1}{2}(1 - P^2)(1 - 3 \cos^2 \theta)] \right\}. \quad (1.13)$$

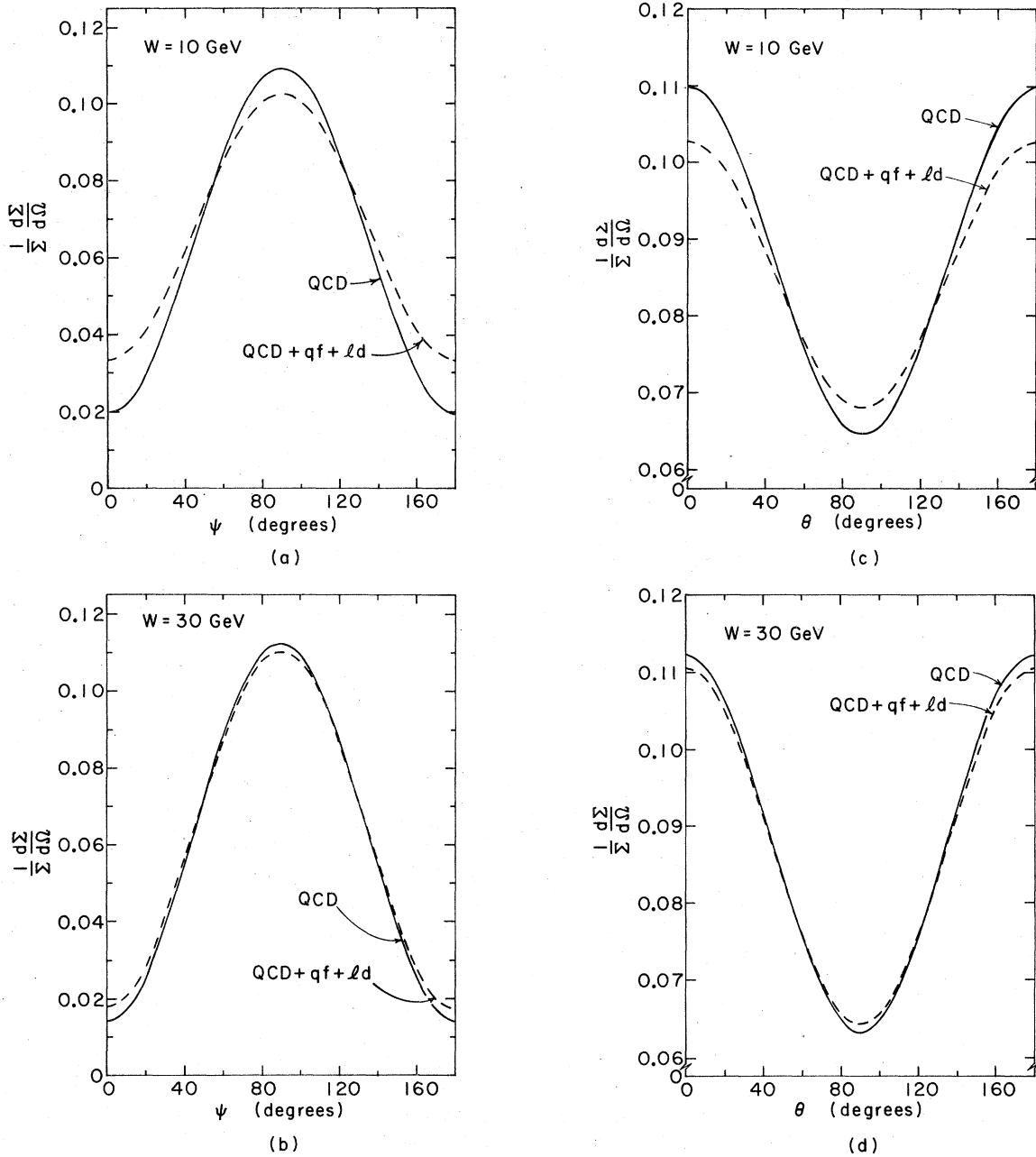


FIG. 4. QCD and the sum of QCD, quark-fragmentation (qf), and heavy-lepton decay (ℓd) contributions to the normalized energy pattern $(1/\Sigma)(d\Sigma/d\Omega)$, with perfectly polarized electron-positron beams of total energy (a) 10 GeV, (b) 30 GeV and unpolarized beams of total energy (c) 10 GeV, (d) 30 GeV. The total hadronic energy cross section Σ is obtained by integrating the energy pattern over the entire solid angular region [cf. Eq. (1.14)]. The curves obtained by neglecting the lepton-decay contributions are not discernibly different from the dashed curves.

Since we now include the effects of heavy-lepton decay, the total energy cross section

$$\Sigma = \int d\Omega \frac{d\Sigma}{d\Omega} \quad (1.14)$$

is no longer simply the total hadronic cross sec-

tion σ_{tot} . The full expression (1.13), normalized by Σ , is plotted for the polarized ($P=1$) and unpolarized ($P=0$) cases in Fig. 4. The heavy lepton is the τ particle¹³ with the parameters¹⁴ $M=1.8$ GeV, $\beta=0.64$, and $\gamma=0.65$. It changes the pattern by an entirely negligible amount ($\sim 1\%$)

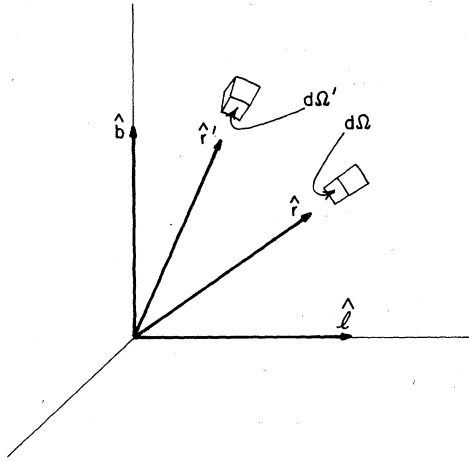


FIG. 5. Geometry for the double-energy-cross-section experiment. The two detectors are positioned in the directions \hat{r} and \hat{r}' while the beam direction is denoted by \hat{l} and the magnetic-field direction by \hat{b} .

which cannot be discerned in the plot.

In the next section, we shall examine a finer-grained measure of the effects of quantum chromodynamics in electron-positron annihilation, the energy-energy correlation cross section. Further

$$\frac{d^2\Sigma}{d\Omega d\Omega'} = \sum_{N=2}^{\infty} \int \prod_{a=1}^N E_a^{-1}(d^3p_a) \frac{d^N\sigma}{E_1^{-1}(d^3p_1) \cdots E_N^{-1}(d^3p_N)} S_N \left[\sum_{b,c=1}^N \frac{E_b E_c}{W^2} \delta(\Omega - \Omega_b) \delta(\Omega' - \Omega_c) \right]. \quad (2.2)$$

Note that terms with $b = c$ are included in this sum. Thus if the two calorimeters are coincident in angle ($\hat{r} = \hat{r}'$), they must both detect the same parcel of energy. The calorimeters are “transparent.” We have included the diagonal terms because energy conservation then yields the normalization

$$\int d\Omega' \frac{d^2\Sigma}{d\Omega d\Omega'} = \frac{d\Sigma}{d\Omega}, \quad (2.3)$$

where $d\Sigma/d\Omega$ is the energy pattern cross section previously defined in Eq. (1.3). [If heavy leptons which decay into hadrons plus a neutrino are included, the normalization (2.3) is no longer strictly valid since the neutrinos are not detected and they carry off part of the energy. However, we shall see shortly that the contribution of heavy leptons is extremely small so that their effects can be neglected.]

The energy pattern cross section is free of infrared mass singularities (at least to order g^2). Hence by Eq. (2.3), the integrated double energy cross section is also free of these singularities. Mass singularities would appear if the diagonal $b = c$ terms were not included. Computing order by order in perturbation theory for massless

quarks and gluons, the δ functions in Eq. (2.2) with $b = c$ give $\delta(\Omega - \Omega')$ with a coefficient that is (infrared) divergent. This divergence should be canceled by other contributions in Eq. (2.2) when one integrates over a small patch of solid angle in either Ω or Ω' which covers $\Omega = \Omega'$. Thus, the double energy cross section should be finite in a distribution-theory sense in the region of nearly collinear detectors ($\Omega = \Omega'$). We demonstrate in Appendix A that, to order g^2 , the cross section is indeed finite in a distribution-theory sense in this region. The perturbation series does not converge uniformly when $\Omega' \rightarrow \Omega$. We expect that, if the series could be summed, this nonuniform behavior would combine with the divergent $\delta(\Omega - \Omega')$ contributions to form a well-defined ordinary function which is sharply peaked near $\Omega' = \Omega$. In perturbation theory, the double energy cross section is also divergent when the detectors are anticollinear ($\Omega' = -\Omega$), and the series also does not converge uniformly when $\Omega' \rightarrow -\Omega$. The lowest-order quark-antiquark production gives a $\delta(\Omega + \Omega')$ angular dependence which acquires a divergent coefficient in higher orders from virtual-gluon exchange. Again, the cross section should be finite in a distribution theory sense in this region of an-

II. ENERGY-ENERGY CORRELATION CROSS SECTION

The double energy cross section¹⁵ can be defined by the following experimental arrangement whose geometry is shown in Fig. 5. A positron and an electron of total energy W annihilate into hadrons. There are two calorimeters, one of solid angle $d\Omega$ in the direction \hat{r} , the other of solid angle $d\Omega'$ in the direction \hat{r}' . The two calorimeters measure the energies dE and dE' which are carried by the hadrons into the solid angles $d\Omega$ and $d\Omega'$ during this single event. The product of the two energies ($dE dE'$) is then summed for many similar events with the sum divided by the integrated luminosity of the beams, $\mathcal{L} \Delta T$, times the squared energy of each collision, W^2 . This procedure defines the double energy cross section

$$\frac{d^2\Sigma}{d\Omega d\Omega'} = \frac{\Sigma_{\text{events}} (dE dE')}{\mathcal{L} \Delta T W^2 d\Omega d\Omega'}. \quad (2.1)$$

In terms of the partial cross section for the process $e^+e^- \rightarrow N$ hadrons, we have, using the notation of Eq. (1.3),

quarks and gluons, the δ functions in Eq. (2.2) with $b = c$ give $\delta(\Omega - \Omega')$ with a coefficient that is (infrared) divergent. This divergence should be canceled by other contributions in Eq. (2.2) when one integrates over a small patch of solid angle in either Ω or Ω' which covers $\Omega = \Omega'$. Thus, the double energy cross section should be finite in a distribution-theory sense in the region of nearly collinear detectors ($\Omega = \Omega'$). We demonstrate in Appendix A that, to order g^2 , the cross section is indeed finite in a distribution-theory sense in this region. The perturbation series does not converge uniformly when $\Omega' \rightarrow \Omega$. We expect that, if the series could be summed, this nonuniform behavior would combine with the divergent $\delta(\Omega - \Omega')$ contributions to form a well-defined ordinary function which is sharply peaked near $\Omega' = \Omega$. In perturbation theory, the double energy cross section is also divergent when the detectors are anticollinear ($\Omega' = -\Omega$), and the series also does not converge uniformly when $\Omega' \rightarrow -\Omega$. The lowest-order quark-antiquark production gives a $\delta(\Omega + \Omega')$ angular dependence which acquires a divergent coefficient in higher orders from virtual-gluon exchange. Again, the cross section should be finite in a distribution theory sense in this region of an-

ticollinearity. This is verified to order g^2 in Appendix A. We also expect that, if the perturbation series were summed, the nonuniform behavior would combine with the divergent $\delta(\Omega + \Omega')$ contributions to produce a well-defined function which is sharply peaked near $\Omega' = -\Omega$. We shall present evidence elsewhere¹⁶ that this does indeed happen.

The double energy cross section $d^2\Sigma/d\Omega d\Omega'$ involves several variables. We shall describe the orientation of the two detection directions \hat{r}, \hat{r}' with polar angles relative to the beam direction \hat{l} and the direction of the magnetic field \hat{b} , defining

$$\begin{aligned} \cos\theta &= \hat{r} \cdot \hat{l}, & \cos\theta' &= \hat{r}' \cdot \hat{l}, \\ \cos\psi &= \hat{r} \cdot \hat{b}, & \cos\psi' &= \hat{r}' \cdot \hat{b}. \end{aligned} \quad (2.4)$$

We also define an angle between the detection directions

$$\cos\chi = \hat{r} \cdot \hat{r}'. \quad (2.5)$$

Since the two directions \hat{r} and \hat{r}' are completely specified by four angles, the five angles $\theta, \theta', \psi, \psi', \chi$ are, of course, not independent. The general form for the energy-energy cross section $d^2\Sigma/d\Omega d\Omega'$ in regard to orientations relative to the beam and magnetic-field directions is obtained easily. The virtual-photon spin density matrix L_{jk} of Eq. (1.5) must appear linearly, contracted with a tensor H_{jk} that characterizes the produced hadronic energies. Since $L_{jk} = L_{kj}$, we can take H_{jk} to be symmetrical in its indices, $H_{jk} = H_{kj}$. Since the directions of the produced hadronic energies are specified by \hat{r} and \hat{r}' , with the cross section unaltered by the interchange $\hat{r} \leftrightarrow \hat{r}'$, H_{jk} must be composed of scalars (depending upon $\cos\chi = \hat{r} \cdot \hat{r}'$, which is even under the interchange) multiplying three possible symmetric matrix

forms. Let us first display the cross section in a manner which makes its positivity obvious. For this purpose, we introduce three symmetrical, positive, mutually orthogonal, projection matrices:

$$P_{jk}^{(1)} = \frac{(\hat{r}_j + \hat{r}'_j)(\hat{r}_k + \hat{r}'_k)}{2(1 + \hat{r} \cdot \hat{r}')}, \quad (2.6a)$$

$$P_{jk}^{(2)} = \frac{(\hat{r}_j - \hat{r}'_j)(\hat{r}_k - \hat{r}'_k)}{2(1 - \hat{r} \cdot \hat{r}')}, \quad (2.6b)$$

and

$$P_{jk}^{(3)} = \delta_{jk} - P_{jk}^{(1)} - P_{jk}^{(2)}. \quad (2.6c)$$

We may now write the double energy cross section in the form

$$\frac{d^2\Sigma}{d\Omega d\Omega'} = \sum_{a=1}^3 A^{(a)}(\hat{r} \cdot \hat{r}') P_{jk}^{(a)} L_{jk}. \quad (2.7)$$

Since the $P_{jk}^{(a)}$ and L_{jk} are symmetrical, positive matrices, the contraction $P_{jk}^{(a)} L_{jk}$ is a positive number. Moreover, since the projections $P_{jk}^{(a)}$ are orthogonal, the numbers $P_{jk}^{(a)} L_{jk}$ for $a=1, 2, 3$ can take on independent values. This is most easily seen for the case of perfect polarization where $L_{jk} = \hat{b}_j \hat{b}_k$. In this case it is clear that \hat{b}_j can be chosen to be orthogonal to any two of the $P_{jk}^{(a)}$. We conclude that the positivity of the cross section requires that each of the scalar coefficients $A^{(a)}(\hat{r} \cdot \hat{r}')$ be non-negative,

$$A^{(a)}(\hat{r} \cdot \hat{r}') \geq 0, \quad a=1, 2, 3. \quad (2.8)$$

Although the structure (2.7) displays the positivity of the cross section in a simple way, it is a cumbersome form for exhibiting the QCD result. Hence we shall replace the matrices $P_{jk}^{(a)}$ with $(2\delta_{jk} - \hat{r}_j \hat{r}_k - \hat{r}'_j \hat{r}'_k)$, $[\delta_{jk}(\hat{r} \cdot \hat{r}') - \frac{1}{2}\hat{r}_j \hat{r}'_k - \frac{1}{2}\hat{r}'_j \hat{r}_k]$, and δ_{jk} . In terms of this new basis, we have

$$\begin{aligned} \frac{d^2\Sigma}{d\Omega d\Omega'} &= \frac{\alpha^2}{2W^2} \sum_f 3Q_f^2 \{ \mathfrak{A}(\chi) [P^2(\sin^2\psi + \sin^2\psi') + \frac{1}{2}(1 - P^2)((1 + \cos^2\theta) + (1 + \cos^2\theta'))] \\ &\quad + \mathfrak{B}(\chi) [P^2(\cos\chi - \cos\psi \cos\psi') + \frac{1}{2}(1 - P^2)(\cos\chi + \cos\theta \cos\theta')] + \mathfrak{C}(\chi) \}. \end{aligned} \quad (2.9)$$

Here we have extracted a convenient overall factor which makes the coefficients $\mathfrak{A}, \mathfrak{B}, \mathfrak{C}$, dimensionless and roughly of order unity. The positivity constraints on these coefficients follows by expressing Eq. (2.9) in the form of Eq. (2.7), and we find the conditions

$$\left(\frac{\alpha^2}{2W^2} \sum_f 3Q_f^2 \right)^{-1} A_1 = (1 - \hat{r} \cdot \hat{r}')(\mathfrak{A} - \frac{1}{2}\mathfrak{B}) + \mathfrak{C} \geq 0, \quad (2.10a)$$

$$\left(\frac{\alpha^2}{2W^2} \sum_f 3Q_f^2 \right)^{-1} A_2 = (1 + \hat{r} \cdot \hat{r}')(\mathfrak{A} + \frac{1}{2}\mathfrak{B}) + \mathfrak{C} \geq 0, \quad (2.10b)$$

and

$$\left(\frac{\alpha^2}{2W^2} \sum_f 3Q_f^2 \right)^{-1} A_3 = 2\mathfrak{A} + \hat{r} \cdot \hat{r}' \mathfrak{B} + \mathfrak{C} \geq 0. \quad (2.10c)$$

The QCD double-energy cross section is calculated in order g^2 in Appendix A, and the result for perfect polarization with the detectors away from collinearity or anticollinearity is presented in Eq. (A29) with ν set equal to 4. This result corresponds to the graphs in Figs. 1(d). Using

$$\zeta = \frac{1}{2}(1 - \cos\chi) \quad (2.11)$$

and comparing Eq. (A29) with Eq. (2.9), we find

$$\alpha^{(\text{QCD})}(\chi) = \frac{\bar{g}(W)^2}{4\pi^2} \frac{1}{12\pi} \frac{1}{1-\zeta} \times \left[\left(\frac{3}{\zeta^5} - \frac{4}{\zeta^4} \right) \ln(1-\zeta) + \frac{3}{\zeta^4} - \frac{5}{2\zeta^3} - \frac{1}{\zeta^2} \right], \quad (2.12)$$

$$\mathfrak{B}^{(\text{QCD})}(\chi) = \frac{\bar{g}(W)^2}{4\pi^2} \frac{1}{12\pi} \frac{1}{1-\zeta} \times \left[\left(\frac{12}{\zeta^5} - \frac{16}{\zeta^4} + \frac{4}{\zeta^3} \right) \ln(1-\zeta) + \frac{12}{\zeta^4} - \frac{10}{\zeta^3} \right], \quad (2.13)$$

and

$$\mathfrak{C}^{(\text{QCD})}(\chi) = 0. \quad (2.14)$$

This cross section diverges when the detectors become collinear ($\chi=0$, $\zeta=0$) or anticollinear ($\chi=\pi$, $\zeta=1$). We have, for $\zeta \rightarrow 0$,

$$\frac{d^2\Sigma^{(\text{QCD})}}{d\Omega d\Omega'} = \alpha^{(\text{QCD})}(\chi) \left(\frac{d\sigma}{d\Omega} + \frac{d\sigma}{d\Omega'} \right) + \mathfrak{B}^{(\text{QCD})}(\chi) \frac{\alpha^2}{2W^2} \sum_f 3Q_f^2 [P^2(\cos\chi - \cos\psi \cos\psi') + \frac{1}{2}(1-P^2)(\cos\chi + \cos\theta \cos\theta')]. \quad (2.19)$$

The fragmentation of the quarks produced in lowest order also contributes to the double energy cross section. This correction is described in detail in Appendix B, and according to Eqs. (B44) and (B76) we have, to within an error of order $1/W^2$ and for $\chi \neq 0, \pi$,

$$\frac{d^2\Sigma^{(\text{qf})}}{d\Omega d\Omega'} = \alpha^{(\text{qf})}(\chi) \left(\frac{d\sigma}{d\Omega} + \frac{d\sigma}{d\Omega'} \right), \quad (2.20)$$

where

$$\alpha^{(\text{qf})}(\chi) = \frac{C}{4\pi} \frac{\langle h_\perp \rangle}{W} \sin^{-3}\chi, \quad (2.21)$$

with C the logarithmic multiplicity coefficient defined in Eq. (1.11) and $\langle h_\perp \rangle$ the average transverse momentum of an emitted hadron. Note that, as in the case of the energy pattern cross section, the fragmentation corrections to the double energy cross section vanish more rapidly as the energy increases ($\propto 1/W$) than does the QCD contribution ($\propto 1/\ln W$). To within an accuracy of order $1/W^2$, there is no quark-fragmentation correction to the terms having the angular dependence with the \mathfrak{B} or \mathfrak{C} coefficients in Eq. (2.9). Moreover, neglecting contributions of order $1/W^2$, the quark-fragmentation contribution to the α coefficient is symmetric under the interchange $\chi \leftrightarrow \pi - \chi$ ($\zeta \leftrightarrow 1 - \zeta$) while the quantum-chromodynamic coefficient $\alpha^{(\text{QCD})}(\chi)$ is markedly asymmetric under this interchange. Thus, measurements of the \mathfrak{B} coef-

$$\alpha^{(\text{QCD})}(\chi) \rightarrow \frac{\bar{g}(W)^2}{4\pi^2} \frac{1}{12\pi} \frac{7}{12\zeta}, \quad (2.15)$$

$$\mathfrak{B}^{(\text{QCD})}(\chi) \rightarrow \frac{\bar{g}(W)^2}{4\pi^2} \frac{1}{12\pi} \frac{1}{3\zeta}, \quad (2.16)$$

and, for $\zeta \rightarrow 1$,

$$\alpha^{(\text{QCD})}(\chi) \rightarrow \frac{\bar{g}(W)^2}{4\pi^2} \frac{1}{12\pi} \frac{1}{1-\zeta} \left[-\ln(1-\zeta) - \frac{1}{2} \right], \quad (2.17)$$

$$\mathfrak{B}^{(\text{QCD})}(\chi) \rightarrow \frac{\bar{g}(W)^2}{4\pi^2} \frac{1}{12\pi} \frac{2}{1-\zeta}. \quad (2.18)$$

As we have just discussed, these singularities cancel in a distribution-theory sense against $\delta(\Omega - \Omega')$, $\delta(\Omega + \Omega')$ contributions that have divergent coefficients. Note that the coefficient of $\alpha(\chi)$ in Eq. (2.9) is just the sum of the lowest-order cross sections (1.6) for each detector. Thus,

efficient and the antisymmetric part of the α coefficient $\alpha(\pi - \chi) - \alpha(\chi)$ should provide precise tests of QCD even at relatively low energies.

The corrections resulting from heavy-lepton decay are also estimated in Appendix B. Since these effects are very small, the rough approximation given in Eq. (B47) suffices. In the high-energy limit, this result reads

$$\frac{d^2\Sigma}{d\Omega d\Omega'} = \alpha^{(\text{ld})}(\chi) \left(\frac{d\sigma}{d\Omega} + \frac{d\sigma}{d\Omega'} \right), \quad (2.22)$$

where

$$\alpha^{(\text{ld})}(\chi) = \frac{2\beta^2\gamma^2}{\pi} \left(\sum_f 3Q_f^2 \right)^{-1} \left(\frac{M}{W} \right)^4 \times \left[\frac{1}{(1-v\cos\chi)^3} + \frac{1}{(1+v\cos\chi)^3} \right], \quad (2.23)$$

with β the semihadronic branching fraction, γ the average fraction of the energy carried off by hadrons, and M the mass of the heavy lepton. Although we have taken the infinite energy limit elsewhere, we have retained the heavy-lepton velocity $v = (1 - 4M^2/W^2)^{1/2}$ in the denominators in Eq. (2.23) since these denominators can become very small. Again, to leading order, the correction to α is symmetric under $\chi \leftrightarrow \pi - \chi$ and there is no contribution to the \mathfrak{B} coefficient.

Figures 6 display our results for the parame-

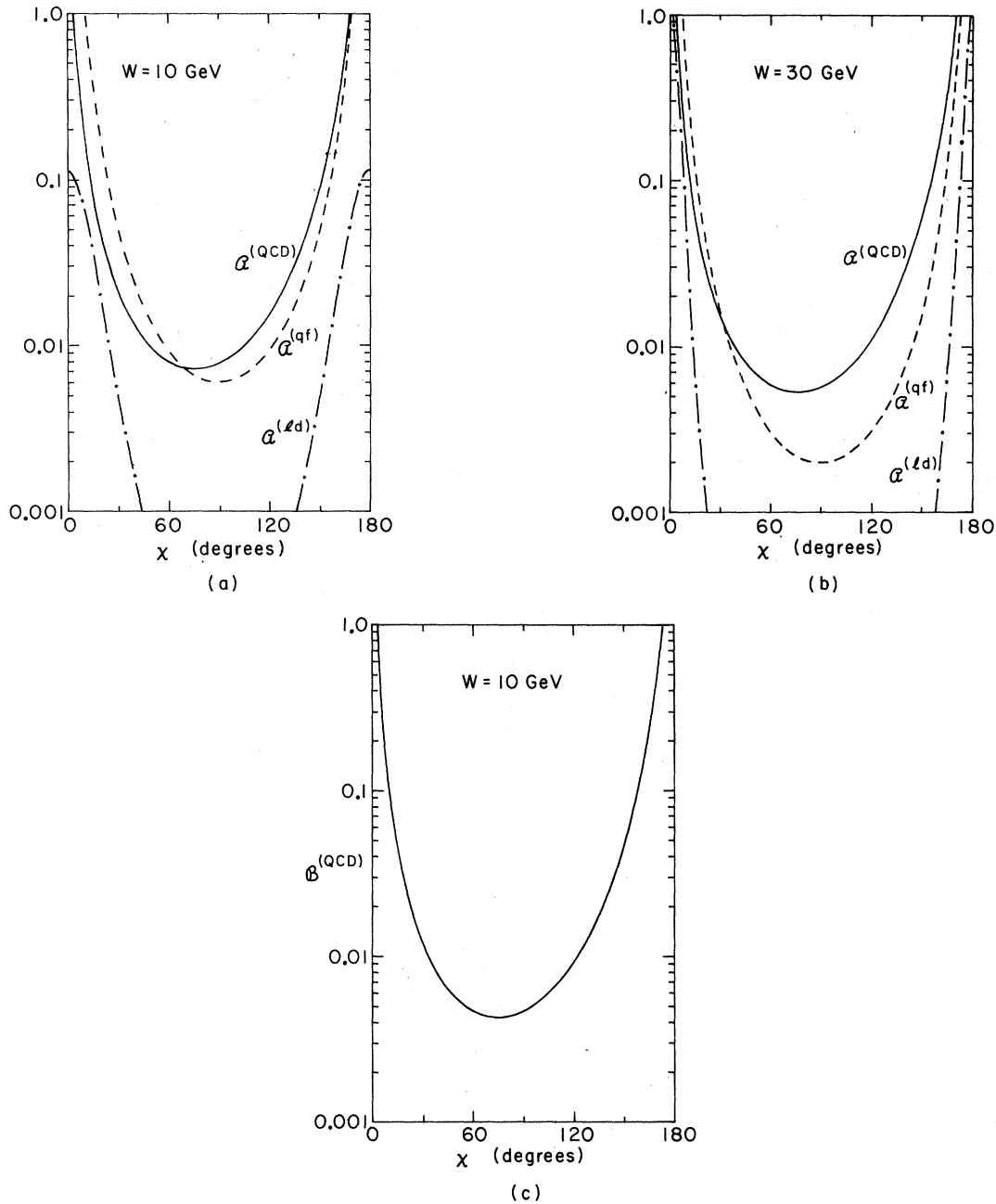


FIG. 6. The QCD, quark fragmentation (qf), and heavy-lepton decay (ld) contributions to the \mathcal{Q} coefficients defined by Eqs. (2.12), (2.21), and (2.23) respectively are plotted as a function of χ for total energy W of (a) 10 GeV and (b) 30 GeV. Notice that the (qf) and (ld) contributions are symmetric about $\chi=90^\circ$ while the QCD behavior is quite asymmetric. (c) The coefficient $\mathcal{B}^{(QCD)}$ defined in Eq. (2.13) as a function of χ for $W=10$ GeV. The plot for $W=30$ is obtained simply by scaling the curve displayed by the factor $\bar{g}(30)^2/\bar{g}(10)^2 \approx 0.73$.

ters^{12,14} $C=2.5$, $\langle h_\perp \rangle=0.3$ GeV, $\beta=0.64$, $\gamma=0.65$, and $M=1.8$ GeV, with the running effective coupling $\bar{g}(W)^2/4\pi^2$ being given by Eq. (1.1) with $N_f=4$ and $\mu=0.5$ GeV. We see that, away from the regions near $\chi=0$ or π where the QCD

perturbation theory breaks down, the heavy-lepton contributions are entirely negligible. Moreover, the quark-fragmentation effects are quite small at $W=30$ GeV and, to within an error of order $1/W^2$, these effects do not contribute to the difference

$$\mathcal{D}(\chi) = \alpha(\pi - \chi) - \alpha(\chi). \quad (2.24)$$

The QCD perturbation contribution to this difference is shown in Fig. 7.

A new measure of the "jet opening angle" is provided by the average

$$\langle \sin^2 \chi \rangle = \frac{1}{\sigma_{\text{tot}}} \int d\Omega d\Omega' \sin^2 \chi \frac{d^2 \Sigma}{d\Omega d\Omega'}. \quad (2.25)$$

Using the general form of Eq. (2.9), we have

$$\langle \sin^2 \chi \rangle = 2\pi \int_0^\pi d\chi \sin^3 \chi \left[2\alpha(\chi) + \cos \chi \mathcal{B}(\chi) + \frac{3}{2} \mathcal{C}(\chi) \right]. \quad (2.26)$$

To exhibit asymmetry in the distribution, we decompose this average into forward ($0 < \chi < \pi/2$) and backward ($\pi/2 < \chi < \pi$) pieces:

$$\langle \sin^2 \chi \rangle_F = 2\pi \int_0^{\pi/2} d\chi \sin^3 \chi \left[2\alpha(\chi) + \cos \chi \mathcal{B}(\chi) + \frac{3}{2} \mathcal{C}(\chi) \right] \quad (2.27a)$$

and

$$\langle \sin^2 \chi \rangle_B = 2\pi \int_{\pi/2}^\pi d\chi \sin^3 \chi \left[2\alpha(\chi) + \cos \chi \mathcal{B}(\chi) + \frac{3}{2} \mathcal{C}(\chi) \right]. \quad (2.27b)$$

Using the QCD results for $\alpha(\chi)$, $\mathcal{B}(\chi)$, and $\mathcal{C}(\chi)$

[Eqs. (2.12), (2.13), and (2.14)], we compute

$$\langle \sin^2 \chi \rangle_F^{(\text{QCD})} = 2 \frac{\bar{g}(W)^2}{4\pi^2} (0.55) \quad (2.28a)$$

and

$$\langle \sin^2 \chi \rangle_B^{(\text{QCD})} = 2 \frac{\bar{g}(W)^2}{4\pi^2} (0.89). \quad (2.28b)$$

This can be compared with the average $\langle \sin^2 \eta \rangle^{(\text{QCD})} = 2 \bar{g}(W)^2 / 4\pi^2$ of Eq. (1.12), an average which identifies a jet opening angle in terms of the broadening of the energy "antenna" pattern. Thus

$$\langle \sin^2 \chi \rangle_F^{(\text{QCD})} = 0.55 \langle \sin^2 \eta \rangle^{(\text{QCD})}, \quad (2.29a)$$

while

$$\langle \sin^2 \chi \rangle_B^{(\text{QCD})} = 0.89 \langle \sin^2 \eta \rangle^{(\text{QCD})}. \quad (2.29b)$$

These results contrast with those produced by the quark-fragmentation process. Introducing Eq. (2.21) [and $\mathcal{B}^{(\text{qt})}(\chi) = 0 = \mathcal{C}^{(\text{qt})}(\chi)$] in Eqs. (2.27a) and (2.27b) and using Eq. (1.10), we find [cf. the discussion of Eq. (B46) in the Appendix]

$$\begin{aligned} \langle \sin^2 \chi \rangle_F^{(\text{qt})} &= \langle \sin^2 \eta \rangle^{(\text{qt})} \\ &= \langle \sin^2 \chi \rangle_B^{(\text{qt})}. \end{aligned} \quad (2.30)$$

Thus the quark-fragmentation contribution is forward-backward symmetric and gives the same result for the two different measures of the jet size. On the other hand, the more complex structure of the quark-antiquark-gluon final state produced in QCD does not have this forward-backward symmetry and yields different results for different measures of the jet size.

III. DISCUSSION AND SUMMARY

Deep-inelastic lepton scattering from nuclear targets provides only a partial test of the theory of quantum chromodynamics, for its complete analysis requires the introduction of arbitrary functions to describe the distribution of constituents within the hadronic target. Electron-positron annihilation avoids such ambiguities since hadrons are absent in the initial state, and various features of this annihilation process have been suggested for possible precise tests of QCD.^{9,11,15} Such features must satisfy several criteria if they are to be useful:

(1) They must be reliably and precisely calculable. This requires freedom from infrared singularities and insensitivity to nonperturbative fragmentation (confinement) effects so that a perturbative analysis is possible.

(2) They must exhibit some special characteristic of QCD, such as the presence of both fermions and gauge vector bosons or the vanishing of the running coupling as the energy increases.

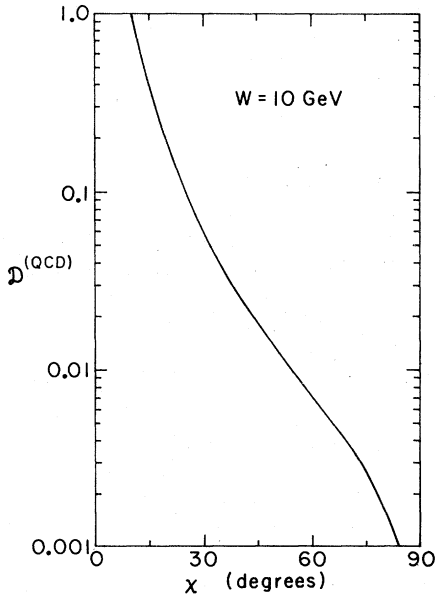


FIG. 7. The difference $\mathcal{D}^{(\text{QCD})}$ defined by Eqs. (2.24) and (2.12) as a function of χ for $W = 10$ GeV. The plot for $W = 30$ GeV is obtained by scaling the curve displayed by the factor $\bar{g}(30)^2 / \bar{g}(10)^2 \approx 0.73$.

(3) They must be accessible to experiment. This constraint argues against studying quantities which are small effects on much larger backgrounds and quantities which are sensitive to the absence of complete (all-particle) data for each annihilation event.

Here and in our previous papers,^{9,15} we have proposed the study of a hierarchy of energy-weighted cross sections to obtain precise tests of quantum chromodynamics. These cross sections involve averages over many events, and they do not require an event-by-event analysis to determine a jet axis as do other proposed tests.^{11(a)} Using the three criteria given above as guidelines, we shall examine the merits of these energy-weighted cross sections for testing quantum chromodynamics.

The first member of this hierarchy is the total cross section, σ_{tot} . It can be rigorously computed by renormalization-group techniques, but the same result is obtained by calculating the total cross section for the production of massless quarks and gluons, using the running effective coupling that vanishes at infinite energy. The latter is the method of asymptotically free perturbation theory. The "antenna-pattern" $d\Sigma/d\Omega$ and the energy-energy correlation cross section $d^2\Sigma/d\Omega d\Omega'$ form the next two members of the hierarchy. We should emphasize that the method of asymptotically free perturbation theory includes the assumption that the nonperturbative fragmentation processes involve limited transverse momenta so that these corrections vanish rapidly as the energy increases. The partial cross sections involve energy weightings, and they should be free from mass singularities due to soft or collinear massless particle production. Thus these quantities, which are outside the usual realm of the renormalization-group and short-distance analysis, should be calculable in the asymptotically free perturbation theory. The antenna-pattern cross section was shown to be finite through second order in our previous work.⁹ The energy-energy cross section is calculated in Appendix A through second order and no mass singularities appear.

The result for this calculation is given by Eqs. (2.12)–(2.14). Experimental studies of the coefficients $\mathfrak{A}(\chi)$ and $\mathfrak{B}(\chi)$, which are proportional to the asymptotically vanishing coupling constant $\bar{g}(W)^2$ and which have properties characteristic of the quark-antiquark-gluon final state, serve as good tests of QCD in accordance with criterion (2). As indicated in criterion (1), these tests should be devised so as to minimize nonperturbative fragmentation effects. The analysis of these effects, presented in Appendix B, is based on the

experimental indication that the momentum of the final-state hadrons transverse to the direction of the parent quark is limited. The contributions of quark fragmentation for the coefficient $\mathfrak{A}(\chi)$ are of order $\langle h_{\perp} \rangle/W$ away from the angular regions near $\chi=0$ or π . These corrections are much smaller at high energies than are the asymptotically free perturbative corrections which vanish only logarithmically. Moreover, it was observed that the leading nonperturbative contributions to $\mathfrak{A}(\chi)$ are symmetric under the interchange $\chi \rightarrow \pi - \chi$ while the perturbative QCD form is quite asymmetric about $\chi = \pi/2$. Thus as the energy increases, the perturbative QCD contribution dominates the values for the antisymmetric part of the \mathfrak{A} coefficient $\mathfrak{D}(\chi) = \mathfrak{A}(\pi - \chi) - \mathfrak{A}(\chi)$, with the fragmentation corrections only of order $1/W^2$. The perturbative QCD contribution also dominates the \mathfrak{B} coefficient at high energies since the nonperturbative corrections here are also of order $1/W^2$. Thus, these measures are particularly insensitive to the effects of fragmentation. The corrections due to heavy-lepton contamination of the hadronic final states are also estimated in Appendix B, using a rough phenomenological model. These corrections are imperceptible [of order $(M/W)^4$] in angular regions away from $\chi=0$ or π . The measurement of the antenna pattern, which we previously suggested as a test of QCD, has larger corrections due to quark fragmentation (of order $\langle h_{\perp} \rangle/W$) and from heavy-lepton decay [of order $(M/W)^2$]. Note that since the quantities which we investigate are averaged over many events, the analysis of fragmentation effects has been considerably simplified, and we have been able to obtain quantitative estimates.

The measures which we have proposed are accessible to experiment as required by point (3). In particular, since the energy-energy cross section is of order $\bar{g}(W)^2$ (plus fragmentation contributions of order $1/W$), it should be straightforward to determine the angular coefficients¹⁷ \mathfrak{A} and \mathfrak{B} which are of the same order. Moreover, at moderate energies the quantities \mathfrak{D} and \mathfrak{B} are dominated by QCD effects since they have small fragmentation contributions of order $1/W^2$. In contrast, measurements of the QCD corrections to the antenna pattern are simpler, but have backgrounds of order g^0 from the lowest-order process and a much greater statistical accuracy is required. Experiments to measure all of these cross sections involve only the detection of energy. They can be performed using only calorimeters. Experiments involving magnetic detectors can be used under the fairly unrestrictive assumption that the *angular* patterns of energy are the same for charged and neutral hadrons. The experimentally

averaged nature of these quantities implies that they are relatively insensitive to experimental fluctuations.

In conclusion, we have presented measures which satisfy three basic criteria for a good test of QCD. Since these measures do not require a detailed event-by-event analysis, they have both calculational and experimental advantages over quantities which involve the event-by-event defini-

tion of a jet axis. Their experimental determination would constitute a precise test of quantum chromodynamics.

ACKNOWLEDGMENTS

We have been aided by conversations with John Rutherford and John Sidles. This work was supported, in part, by the U.S. Department of Energy.

APPENDIX A

Here we shall give some of the details of the calculation of the second-order QCD energy-energy cross section, formula (2.9) in the text. Moreover, we shall prove that this formula, suitably regulated and augmented by the collinear and anticollinear δ -function terms described in the text, is finite in a distribution-theory sense. This proof is greatly facilitated by using a dimensional-continuation scheme.¹⁸

The general definition of the energy-energy angular correlation cross section presented in the text, Eq. (2.2), may be written equivalently as

$$\frac{d^2\Sigma}{d\Omega d\Omega'} = \sum_{N=2}^{\infty} \int \left[\prod_{a=1}^N \frac{(d^3p_a)}{(2\pi)^3 2E_a} \right] (2\pi)^4 \delta^{(4)}(p_1 + p_2 + \dots + p_N - q) |T_N|^2 \frac{1}{2W^2} \sum_{b,c=1}^N \frac{E_b E_c}{W W} \delta(\Omega - \Omega_b) \delta(\Omega' - \Omega_c). \quad (\text{A1})$$

The N -particle production amplitude T_N contains appropriate factorials so that identical particles are not overcounted in the integration over the final phase space. The four-momentum of the virtual photon is denoted by q^μ , with

$$q = l + \bar{l}, \quad (\text{A2})$$

where l^μ and \bar{l}^μ are the four-momenta of the electron and positron. We work in the laboratory frame which is the center-of-mass frame of the annihilation. Thus

$$q^\mu = (W, \vec{0}). \quad (\text{A3})$$

As discussed in the text, the sum over the particle indices b and c in Eq. (A1) runs over all the N^2 possibilities, including the N terms with $b = c$. Thus, the energy of the same particle will be counted by both detectors when they are aligned; they are "transparent" calorimeters. This definition is necessary to achieve an infrared-finite energy-energy cross section. If we integrate the energy-energy cross section over the entire range of one of the solid angles, say over $d\Omega'$, then with the unrestricted sum over c , the energy-conserving δ function for N particles gives

$$\int d\Omega' \sum_{c=1}^N \delta(\Omega' - \Omega_c) \frac{E_c}{W} = \frac{1}{W} \sum_{c=1}^N E_c = 1. \quad (\text{A4})$$

Hence

$$\int d\Omega' \frac{d^2\Sigma}{d\Omega d\Omega'} = \frac{d\Sigma}{d\Omega}, \quad (\text{A5})$$

where $d\Sigma/d\Omega$ is the single-energy cross section discussed in the text. We have proved in our

previous work that this single-energy cross section in QCD has no infrared mass singularities to second order, and we expect that it is devoid of such mass singularities to all orders.

We shall use the general definition (A1) to calculate the double-energy cross section for the second-order QCD processes shown in Fig. 1. We are interested in the limit where both the quarks and the gluons are massless, a limit where separate pieces of the calculation become singular. We shall regulate these potential singularities by performing our calculations in a space-time of dimensionality $\nu > 4$, keeping the quarks and gluons always to have zero mass. The limit $\nu \rightarrow 4$ will be taken only after all contributions to the cross section have been added together. In our space-time with ν dimensions we have a metric tensor $g_{\mu\nu}$ with signature $(-, +, +, \dots, +)$ and Dirac matrices obeying $\{\gamma_\mu, \gamma_\nu\} = -2g_{\mu\nu}$. The 4×4 γ matrices for ordinary four-space must be increased in their dimensionality as the dimensions of space-time are increased. However, we shall adopt the fiction that $\text{tr}(\gamma^0)^2 = \text{tr} 1 = 4$. This ruse is permissible since all our expressions will involve a single, overall trace in the γ -matrix space, with the trace constrained to give $\text{tr} 1 = 4$ when $\nu = 4$. With $\nu \neq 4$, the overall trace in a consistent definition would produce a dimension-dependent factor $\text{tr} 1 = f(\nu)$, but the entire expression which multiplies this factor is finite at $\nu = 4$, and hence $f(\nu)$ may be replaced by $f(4) = 4$.

We turn now to the single-gluon-emission process depicted in Fig. 1(d). The squared matrix element in ν dimensions has the form

$$|T_3|^2 = \frac{e^4 \kappa^{8-2\nu}}{W^2} L_{\mu\nu} H^{\mu\nu}. \quad (\text{A6})$$

Here a scale mass κ has been introduced to keep the electric charge e dimensionless. The virtual-photon spin-density tensor $L_{\mu\nu}$ is obtained from the square of the leptonic current¹⁹

$$\frac{1}{W} \bar{v}(\bar{l}) \gamma_\mu u(l),$$

averaged with the density matrix for the spins of the e^+e^- . Our calculation is simplified somewhat by assuming that the e^+e^- system is perfectly polarized along the magnetic field direction \hat{b} , a direction perpendicular to that of the electron, \hat{l} . In this case, $L_{\mu\nu}$ has only the spatial components

$$L_{kl} = \hat{b}_k \hat{b}_l. \quad (\text{A7})$$

[Cf. Eq. (1.5) of the text. As explained there in detail, the result for general polarization can always be obtained from that for the perfect polarization, Eq. (A7).]

The normalization of the QCD coupling constant g is specified by the interaction Lagrangian

$$\mathcal{L}_I = \kappa^{2-\nu/2} g \bar{q} \gamma_\mu \lambda_a q A_a^\mu, \quad (\text{A8})$$

where the color SU(3) generating matrices λ_a have an isospin normalization, so that, for example

$$\lambda_3 = \begin{pmatrix} \frac{1}{2} & 0 & 0 \\ 0 & -\frac{1}{2} & 0 \\ 0 & 0 & 0 \end{pmatrix}. \quad (\text{A9})$$

Again the mass scale κ has been introduced to keep the QCD coupling constant g dimensionless. We denote the ν -momenta of the produced quark and antiquark by p and \bar{p} and that of the produced gluon by k . Thus, momentum conservation reads

$$p + \bar{p} + k = q. \quad (\text{A10})$$

The fractional charge of a quark of flavor f is given by Q_f . Using these conventions, the hadron tensor $H^{\mu\nu}$ is given by

$$\begin{aligned} H^{\mu\nu} = \kappa^{4-\nu} \sum_f \text{tr} \left[g \lambda_a \gamma^\sigma \frac{\gamma \cdot (p+k)}{(p+k)^2} Q_f \gamma^\mu - Q_f \gamma^\mu \frac{\gamma \cdot (\bar{p}+k)}{(\bar{p}+k)^2} g \lambda_a \gamma^\sigma \right] \gamma \cdot \bar{p} \\ \times \left[Q_f \gamma^\nu \frac{\gamma \cdot (p+k)}{(p+k)^2} g \lambda_a \gamma^\sigma - g \lambda_a \gamma^\sigma \frac{\gamma \cdot (\bar{p}+k)}{(\bar{p}+k)^2} Q_f \gamma^\nu \right] \gamma \cdot p. \end{aligned} \quad (\text{A11})$$

Evaluating the trace and displaying the result in a manner which makes current conservation manifest,

$$q_\mu H^{\mu\nu} = 0 = H^{\mu\nu} q_\nu, \quad (\text{A12})$$

we find

$$\begin{aligned} H^{\mu\nu} = 32 \kappa^{4-\nu} g^2 \sum_f Q_f^2 \left\{ \frac{1}{(\bar{p}+k)^2} \frac{1}{(p+k)^2} \left[(q^2 g^{\mu\nu} - q^\mu q^\nu) q^2 + [\Delta^\mu \Delta^\nu q^2 - (q^\mu \Delta^\nu + \Delta^\mu q^\nu) q \cdot \Delta + g^{\mu\nu} (q \cdot \Delta)^2] \right. \right. \\ \left. \left. + [k^\mu k^\nu q^2 - (q^\mu k^\nu + k^\mu q^\nu) q \cdot k + g^{\mu\nu} (q \cdot k)^2] [1 + (\nu - 4)] \right\} \right. \\ \left. - (g^{\mu\nu} q^2 - q^\mu q^\nu) \left[\frac{1}{(p+k)^2} + \frac{1}{(\bar{p}+k)^2} \right] \right\}, \end{aligned} \quad (\text{A13})$$

where $\Delta = \bar{p} - p$. This expression can be simplified when it is contracted with the lepton tensor $L_{\mu\nu}$; factors which are proportional to q^μ or q^ν can be neglected since they are orthogonal to $L_{\mu\nu}$, which is the statement that the leptonic current is conserved. Thus, effectively,

$$H^{\mu\nu} = 64 \kappa^{4-\nu} g^2 \sum_f Q_f^2 \frac{1}{W-2E} \frac{1}{W-2\bar{E}} \left\{ [E^2 + \bar{E}^2 + (\frac{1}{2}\nu - 2)\omega^2] g^{\mu\nu} - p^\mu p^\nu - \bar{p}^\mu \bar{p}^\nu - (\frac{1}{2}\nu - 2) k^\mu k^\nu \right\}, \quad (\text{A14})$$

where

$$p^\mu = E(1, \hat{p}), \quad \bar{p}^\mu = \bar{E}(1, \hat{\bar{p}}), \quad k^\mu = \omega(1, \hat{k}), \quad (\text{A15})$$

and

$$W = E + \bar{E} + \omega. \quad (\text{A16})$$

Contracting the hadronic tensor, Eq. (A14) with the leptonic tensor (A7) yields, according to Eq. (A6), a squared amplitude for the production of a quark-antiquark-gluon final state given by

$$|T_3|^2 = 64e^4 g^2 \kappa^{12-3\nu} \frac{1}{W^2} \sum_f Q_f^2 \frac{1}{W-2E} \frac{1}{W-2\bar{E}} \quad (\text{A17})$$

$$\times \{E^2[1 - (\hat{p} \cdot \hat{b})^2] + \bar{E}^2[1 - (\hat{p} \cdot \hat{b})^2] + (\frac{1}{2}\nu - 2)\omega^2[1 - (\hat{k} \cdot \hat{b})^2]\}.$$

The general definition of the double energy cross section, Eq. (A1), must be extended to a ν -dimensional space-time by writing the phase-space integrals for ν dimensions rather than four dimensions. Thus we write

$$\frac{d^2\Sigma}{d\Omega d\Omega'} = \sum_{N=2}^{\infty} \int \left[\prod_{a=1}^N \frac{(a^{\nu-1} p_a)}{(2\pi)^{\nu-1} 2E_a} \right] (2\pi)^\nu \delta^{(\nu)}(p_1 + p_2 + \cdots + p_N - q) |T_N^{\psi}|^2 \frac{1}{2W^2} \quad (\text{A18})$$

$$\times \sum_{b,c=1}^N \frac{E_b}{W} \frac{E_c}{W} \delta^{(\nu-2)}(\Omega - \Omega_b) \delta^{(\nu-2)}(\Omega' - \Omega_c).$$

We may now apply the dimensionally continued formula (A18) for the double energy cross section to the production of a quark-antiquark-gluon final state in order g^2 . We consider first the partial cross section $d^2\Sigma^{(q\bar{q})}/d\Omega d\Omega'$, where the quark and antiquark are detected with $\Omega = \Omega_q$, $\Omega' = \Omega_{\bar{q}}$ or $\Omega = \Omega_{\bar{q}}$, $\Omega' = \Omega_q$. Inserting Eq. (A17) in Eq. (A18) we find after some calculation that

$$\frac{d^2\Sigma^{(q\bar{q})}}{d\Omega d\Omega'} = \frac{\alpha^2}{24\pi W^2} \frac{\kappa^{12-3\nu} W^{2\nu-8}}{(4\pi)^{2\nu-8}} \sum_f 3Q_f^2 \frac{g^2}{4\pi^2} \frac{|\Gamma(\nu)\Gamma(\nu-1)|}{\Gamma(2\nu-2)}$$

$$\times \frac{1}{1-\zeta} \left[\frac{1}{2} F(\nu, \nu-2; 2\nu-2; \zeta)(\sin^2\psi + \sin^2\psi') \right. \\ \left. + \frac{(\nu-4)}{(\nu-1)} F(\nu-1, \nu-1; 2\nu-2; \zeta)(\cos\chi - \cos\psi \cos\psi') \right], \quad (\text{A19})$$

where $F(a, b; c; z)$ is the usual hypergeometric function.²⁰ Here

$$\zeta = \frac{1}{2}(1 - \cos\chi), \quad (\text{A20})$$

where χ is the angle between the two detectors, while ψ and ψ' are the angles between the detector directions and the magnetic-field direction. Specifying the detector directions by \hat{r} and \hat{r}' , we have

$$\cos\chi = \hat{r} \cdot \hat{r}' \quad (\text{A21})$$

and

$$\cos\psi = \hat{b} \cdot \hat{r}, \quad \cos\psi' = \hat{b} \cdot \hat{r}'. \quad (\text{A22})$$

This geometry is illustrated in Fig. 8. Since the hypergeometric functions approach 1 as $\zeta \rightarrow 0$, we see that the cross section (A19) is finite at $\zeta = 0$ ($\chi = 0$) when the energy detectors are coincident. This is to be expected since, when the quark and antiquark are aligned, the gluon must carry half the energy in the opposite direction. Thus the gluon is neither soft nor collinear with another massless particle and no divergence should appear. On the other hand, the cross section (A19) diverges at $\zeta = 1$ ($\chi = \pi$), where the quark and antiquark emerge anticollinearly. We can isolate divergent pieces by using the series expansion²⁰

$$F(a, b; a+b; z) = \frac{\Gamma(a+b)}{\Gamma(a)^2 \Gamma(b)^2} \sum_{n=0}^{\infty} \frac{\Gamma(a+n)\Gamma(b+n)}{(n!)^2} [-\ln(1-z) + 2\psi(n+1) - \psi(a+n) - \psi(b+n)](1-z)^n \quad (\text{A23})$$

and keeping only the $n=0$ term. Noting that as $\zeta \rightarrow 1$, $\cos\psi' \rightarrow -\cos\psi$, we find that the cross section in this limit is given by

$$\frac{d^2\Sigma^{(q\bar{q})}}{d\Omega d\Omega'} \Big|_{\zeta \rightarrow 1} \approx \frac{\alpha^2}{24\pi W^2} \frac{\kappa^{12-3\nu} W^{2\nu-8}}{(4\pi)^{2\nu-8}} \sum_f 3Q_f^2 \frac{g^2}{4\pi^2} \frac{1}{1-\zeta} \left[2 \ln \frac{1}{1-\zeta} - \frac{17}{3} + \left(\frac{88}{9} - \frac{4}{3}\pi^2\right) \left(\frac{1}{2}\nu - 2\right) \right] \sin^2\psi. \quad (\text{A24})$$

Here we have retained all the terms which, while integrable in $\nu > 4$ dimensions, either produce divergent integrals as $\nu \rightarrow 4$ or integrals that are finite at $\nu = 4$ but which are independent of the integration range. The latter involve $(\nu-4)(1-\zeta)^{-1}$ whose limit is essentially $\delta(1-\zeta)$.

Let us turn now to the contribution $d^2\Sigma^{(qg)}/d\Omega d\Omega'$ which arises when the quark (antiquark) and the gluon are detected, i.e., when $\Omega = \Omega_q$ ($\Omega = \Omega_{\bar{q}}$), $\Omega' = \Omega_g$, or $\Omega' = \Omega_q$ ($\Omega' = \Omega_{\bar{q}}$), $\Omega = \Omega_g$. These configurations give

$$\begin{aligned} \frac{d^2\Sigma^{(qg)}}{d\Omega d\Omega'} &= \frac{\alpha^2}{24\pi W^2} \frac{\kappa^{12-3\nu} W^{2\nu-8}}{(4\pi)^{2\nu-8}} \sum_f 3Q_f^2 \frac{g^2}{4\pi^2} \frac{\Gamma(\nu-2)\Gamma(\nu-1)}{\Gamma(2\nu-3)} \frac{1}{\zeta(1-\zeta)} \\ &\times \left[\left(\frac{2(\nu-1)}{(\nu-3)} + \frac{1}{2}(\nu-2) \right) F(\nu-3, \nu-1; 2\nu-3; \zeta)(\sin^2\psi + \sin^2\psi') \right. \\ &\left. + 4F(\nu-2, \nu-2; 2\nu-3; \zeta)(\cos\chi - \cos\psi \cos\psi') \right]. \end{aligned} \tag{A25}$$

This expression is singular at both $\zeta=0$ and $\zeta=1$, with

$$\frac{d^2\Sigma^{(qg)}}{d\Omega d\Omega'} \underset{\zeta \rightarrow 0}{\approx} \frac{\alpha^2}{24\pi W^2} \frac{\kappa^{12-3\nu} W^{2\nu-8}}{(4\pi)^{2\nu-8}} \sum_f 3Q_f^2 \frac{g^2}{4\pi^2} \frac{1}{\zeta} \left[\frac{3}{2} - \frac{37}{6}(\frac{1}{2}\nu - 2) \right] \sin^2\psi \tag{A26}$$

and

$$\frac{d^2\Sigma^{(qg)}}{d\Omega d\Omega'} \underset{\zeta \rightarrow 1}{\approx} \frac{\alpha^2}{24\pi W^2} \frac{\kappa^{12-3\nu} W^{2\nu-8}}{(4\pi)^{2\nu-8}} \sum_f 3Q_f^2 \frac{g^2}{4\pi^2} \frac{1}{1-\zeta} \left[\frac{3}{3} - \frac{52}{9}(\frac{1}{2}\nu - 2) \right] \sin^2\psi, \tag{A27}$$

where the $\zeta \rightarrow 1$ limit follows from the relationship²⁰

$$\lim_{z \rightarrow 1} F(a, b; a+b+1; z) = \frac{\Gamma(a+b+1)}{\Gamma(a+1)\Gamma(b+1)}. \tag{A28}$$

Again, these are the contributions which are integrable in $\nu > 4$ dimensions but whose integral over an arbitrarily small region either diverges or approaches a constant when ν approaches 4.

The limit $\nu \rightarrow 4$ can be taken in Eqs. (A19) and (A25) if ζ is kept away from $\zeta=0$ or $\zeta=1$. In this case the hypergeometric functions reduce to simple logarithms and algebraic functions. These results can be combined with the limits displayed in Eqs. (A24), (A26), and (A27) to obtain an expression for the total real emission cross section that is valid for all values of ζ in the $\nu \rightarrow 4$ limit:

$$\begin{aligned} \frac{d^2\Sigma^{(\text{real})}}{d\Omega d\Omega'} &= \frac{d^2\Sigma^{(q\bar{q})}}{d\Omega d\Omega'} + \frac{d^2\Sigma^{(qg)}}{d\Omega d\Omega'} \\ &= \frac{\alpha^2}{24\pi W^2} \frac{\kappa^{12-3\nu} W^{2\nu-8}}{(4\pi)^{2\nu-8}} \sum_f 3Q_f^2 \frac{g^2}{4\pi^2} \frac{1}{1-\zeta} \left\{ \left[\left(\frac{3}{\zeta^5} - \frac{4}{\zeta^4} \right) \ln(1-\zeta) + \frac{3}{\zeta^4} - \frac{5}{2\zeta^3} - \frac{1}{\zeta^2} \right. \right. \\ &\quad \left. \left. + \left(-\frac{37(1-\zeta)}{12\zeta} + 2 - \frac{2}{3}\pi^2 \right) (\frac{1}{2}\nu - 2) \right] (\sin^2\psi + \sin^2\psi') \right. \\ &\quad \left. + \left[\left(\frac{12}{\zeta^5} - \frac{16}{\zeta^4} + \frac{4}{\zeta^3} \right) \ln(1-\zeta) + \frac{12}{\zeta^4} - \frac{10}{\zeta^3} \right] (\cos\chi - \cos\psi \cos\psi') \right\}. \end{aligned} \tag{A29}$$

We should remark that such a simple form can be obtained because the hypergeometric functions [Eqs. (A23) and (A28)] have uniform limits when $\zeta \rightarrow 1$ or $\zeta \rightarrow 0$ and $\nu \rightarrow 4$. This would not have been possible, for example, with a function involving $(1-\zeta)^{\nu-4}$ whose expansion in powers of $\nu-4$ is accompanied by powers of $\ln(1-\zeta)$. In such cases, the entire series must be kept since successive terms give comparable contributions when one integrates over ζ .

The complete energy-energy cross section will be well defined in a distribution-theory sense if its integrals over small angular regions in Ω or Ω' are finite in the limit $\nu \rightarrow 4$. This requires that the singularities at $\zeta=0$ and $\zeta=1$ displayed

above cancel against singularities arising from the order- g^2 vertex correction due to the virtual-gluon exchange illustrated in Fig. 1(b) and against the further singularities appearing at $\zeta=0$ due to the real emission process with only one particle passing through both "transparent" detectors. The vertex singularities appear as a factor multiplying the zeroth-order cross section and thus contribute in the anticollinear orientation $\zeta=1$. The vertex singularities also contribute to the collinear orientation because of the "transparent" detector character of the energy-energy cross section. To establish this cancellation, we need an expression for the $(\nu-2)$ -dimensional element of solid angle appropriate to a ν -dimensional

space-time,

$$\int d^{\nu-3}\Omega' = \frac{2\pi^{\nu/2-1}}{\Gamma(\frac{1}{2}\nu-1)}. \quad (\text{A31})$$

$$\begin{aligned} d^{\nu-2}\Omega' &= \sin^{\nu-3}\chi d\chi d^{\nu-3}\Omega' \\ &= 2[4\xi(1-\xi)]^{\nu/2-2} d\xi d^{\nu-3}\Omega' \end{aligned} \quad (\text{A30})$$

and

$$\begin{aligned} \int_{1-\xi_0 \leq \xi \leq 1} d^{\nu-2}\Omega' \frac{d^2\Sigma^{(\text{real})}}{d\Omega d\Omega'} &= \frac{\alpha^2}{6W^2} \frac{\kappa^{12-3\nu} W^{2\nu-8}}{(4\pi)^{(3/2)\nu-6}} \sum_f 3Q_f^2 \frac{g^2}{4\pi^2} \\ &\times \left[\frac{2}{(\frac{1}{2}\nu-2)^2} + \frac{(-3+2\gamma)}{(\frac{1}{2}\nu-2)} + (-\ln^2\xi_0 - 3\ln\xi_0 - \frac{3}{2}\pi^2 + \gamma^2 - 3\gamma + 4) \right] \sin^2\psi \end{aligned} \quad (\text{A32})$$

and

$$\int_{0 \leq \xi \leq \xi_0} d^{\nu-2}\Omega' \frac{d^2\Sigma^{(\text{real})}}{d\Omega d\Omega'} = \frac{\alpha^2}{6W^2} \frac{\kappa^{12-3\nu} W^{2\nu-8}}{(4\pi)^{(3/2)\nu-6}} \sum_f 3Q_f^2 \frac{g^2}{4\pi^2} \left[\frac{3}{2} \frac{1}{(\frac{1}{2}\nu-2)} + \left(\frac{3}{2} \ln\xi_0 + \frac{3}{2}\gamma - \frac{37}{6} \right) \right] \sin^2\psi, \quad (\text{A33})$$

where $\gamma = 0.577\dots$ is Euler's constant. These are the terms which must cancel the divergent $\delta(\Omega - \Omega')$ and $\delta(\Omega + \Omega')$ contributions mentioned above.

The "transparent" detector contribution for the real gluon emission process is obtained by inserting $|T_3|^2$ given by Eq. (A17) into Eq. (A18) and extracting only those terms with $b=c$, terms which have an overall factor of $\delta(\Omega - \Omega')$. A straightforward calculation yields

$$\begin{aligned} \frac{d^2\Sigma^{(\text{trans})}}{d\Omega d\Omega'} &= \frac{\alpha^2}{6W^2} \frac{\kappa^{12-3\nu} W^{2\nu-8}}{(4\pi)^{(3/2)\nu-6}} \sum_f 3Q_f^2 \frac{g^2}{4\pi^2} \delta^{(\nu-2)}(\Omega - \Omega') \\ &\times \left\{ \left[\frac{2}{(\frac{1}{2}\nu-2)^2} + \frac{(-\frac{9}{2} + \gamma)}{(\frac{1}{2}\nu-2)} + \left(\gamma^2 - \frac{9}{2}\gamma + \frac{353}{24} - \frac{7}{6}\pi^2 \right) \right] \sin^2\psi + \frac{2}{3} (3\cos^2\psi - 1) \right\}, \end{aligned} \quad (\text{A34})$$

where we have retained only those terms which are nonvanishing for $\nu=4$.

The order- g^2 correction to the vertex, illustrated in Fig. 1(b), appears in ν dimensions as

$$\Gamma^\mu(-\bar{p}, p) = -i\kappa^{4-\nu} \int \frac{(d^\nu k)}{(2\pi)^\nu} \frac{1}{k^2} g\lambda_a \gamma^\sigma \frac{\gamma \cdot (-\bar{p} + k)}{(-\bar{p} + k)^2} \gamma^\mu \frac{\gamma \cdot (p + k)}{(p + k)^2} g\lambda_a \gamma_\sigma. \quad (\text{A35})$$

We shall calculate this vertex on the zero mass shell with, effectively, $\gamma\bar{p} = 0 = \gamma p$. We perform some simple γ_μ and λ_a matrix algebra and write the vertex in the form

$$\begin{aligned} \Gamma^\mu(-\bar{p}, p) &= -i\frac{4}{3}g^2\kappa^{4-\nu} \int \frac{(d^\nu k)}{(2\pi)^\nu} \frac{1}{k^2} \left(\frac{1}{k^2 - 2\bar{p} \cdot k} \frac{1}{k^2 + 2p \cdot k} \left\{ \gamma^\mu \left[-4\bar{p} \cdot p - \left(4 - \frac{(\nu-2)^2}{\nu} \right) (\bar{p} - p) \cdot k \right] \right. \right. \\ &\quad \left. \left. + \frac{2}{\nu} (\nu-2)(\gamma^\mu k^2 - \nu k^\mu \gamma \cdot k) + 4(\bar{p} - p)^\mu \gamma \cdot k \right\} \right. \\ &\quad \left. + \left[\frac{1}{k^2 - 2\bar{p} \cdot k} + \frac{1}{k^2 + 2p \cdot k} \right] \frac{1}{2\nu} (\nu-2)^2 \gamma^\mu \right). \end{aligned} \quad (\text{A36})$$

The integration converges in the region $4 < \nu < 6$ for all the terms except those enclosed in the last square brackets. The latter terms are both infrared and ultraviolet divergent at $\nu=4$, and there is no value of ν for which they give a convergent integral. Thus, these terms must be separately regulated, for example by the replacement $1/k^2 \rightarrow 1/k^2 - 1/(k^2 + \Lambda^2)$. However, as we shall now prove, they are exactly canceled by the wave-function renormalization of the vertex.²¹

The second-order self-energy correction to the quark propagator corresponding to the graph shown in Fig. 9 is given by

$$\begin{aligned}\Sigma(p) &= -i\kappa^{4-\nu} \int \frac{(d^{\nu}k)}{(2\pi)^{\nu}} \frac{1}{k^2} \frac{1}{(p+k)^2} g\lambda_a \gamma^{\sigma} \gamma \cdot (p+k) g\lambda_a \gamma_{\sigma} \\ &= -i\frac{4}{3} g^2 (\nu-2) \kappa^{4-\nu} \int \frac{(d^{\nu}k)}{(2\pi)^{\nu}} \frac{1}{k^2} \frac{1}{(p+k)^2} \gamma \cdot (p+k).\end{aligned}\quad (\text{A37})$$

Here it is to be understood that the gluon propagator $1/k^2$ has been suitably regulated so as to make the integral converge. Now with symmetric k integration we have, effectively,

$$\begin{aligned}\frac{1}{(p+k)^2} \gamma \cdot k &= \frac{1}{2} \left[\frac{1}{(p+k)^2} - \frac{1}{(p-k)^2} \right] \gamma \cdot k \\ &= \frac{-2p \cdot k}{(p+k)^2 (p-k)^2} \gamma \cdot k.\end{aligned}\quad (\text{A38})$$

Moreover, after combining denominators, translating k , and integrating symmetrically,

$$(p \cdot k)(\gamma \cdot k) \rightarrow \frac{1}{\nu} (\gamma \cdot p) k^2 + (\gamma \cdot p) p^2 \dots \quad (\text{A39})$$

We are interested only in evaluating the quark wave-function renormalization constant δZ , which is the negative of the coefficient of γp in $\Sigma(p)$ at $p^2=0$,

$$\delta Z \gamma p = -\Sigma(p) \Big|_{p^2=0}. \quad (\text{A40})$$

Hence the $p^2 \dots$ terms in Eq. (A39) can be neglected, and effectively,

$$\begin{aligned}\frac{1}{(p+k)^2} \gamma \cdot k &= -\frac{1}{\nu} \left(\frac{1}{k^2 + 2p \cdot k} + \frac{1}{k^2 - 2p \cdot k} \right) \gamma \cdot p \\ &= -\frac{2}{\nu} \frac{1}{k^2 + 2p \cdot k} \gamma \cdot p.\end{aligned}\quad (\text{A41})$$

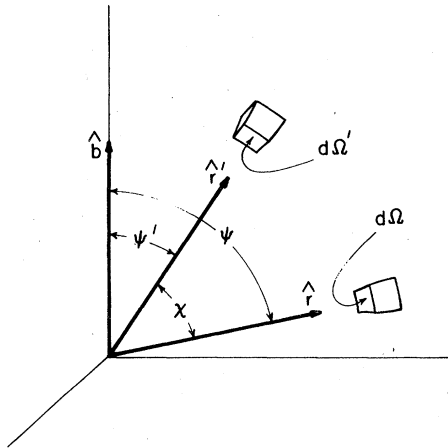


FIG. 8. Geometry for the energy-energy cross-section experiment for the case of perfectly polarized e^+e^- beams. The two detectors are stationed in directions \hat{r} and \hat{r}' with relative angle χ . These detector directions are respectively at angles ψ and ψ' relative to the magnetic field direction (the polarization direction) denoted by \hat{b} .

Accordingly,

$$\begin{aligned}\delta Z &= i\frac{4}{3} g^2 \frac{(\nu-2)^2}{\nu} \kappa^{4-\nu} \\ &\times \int \frac{(d^{\nu}k)}{(2\pi)^{\nu}} \frac{1}{k^2} \frac{1}{k^2 + 2p \cdot k}.\end{aligned}\quad (\text{A42})$$

With $p^2=0$, this (suitably regulated) integral is otherwise independent of p^μ . Thus, we may write the renormalized vertex as

$$\begin{aligned}\Gamma_{\text{ren}}^\mu &= \Gamma^\mu + \delta Z \gamma^\mu \\ &= \Gamma^\mu + i\frac{4}{3} g^2 \kappa^{4-\nu} \\ &\times \int \frac{(d^{\nu}k)}{(2\pi)^{\nu}} \frac{1}{k^2} \left(\frac{1}{k^2 - 2\bar{p} \cdot k} + \frac{1}{k^2 + 2p \cdot k} \right) \\ &\times \frac{1}{2\nu} (\nu-2)^2 \gamma^\mu.\end{aligned}\quad (\text{A43})$$

and we see that the badly behaved term in the vertex integral (A36) is precisely canceled by the wave-function renormalization.

The renormalized vertex can now be evaluated by standard methods, and we obtain

$$\Gamma_{\text{ren}}^\mu(-\bar{p}, p) = \gamma^\mu I(2\bar{p} \cdot p), \quad (\text{A44})$$

where

$$\begin{aligned}I(2\bar{p} \cdot p) &= \frac{4}{3} g^2 \left(\frac{2\bar{p} \cdot p}{\kappa^2} \right)^{\nu/2-2} \frac{1}{(4\pi)^{\nu/2}} \\ &\times [\Gamma(\nu/2 - 2)]^2 \frac{\Gamma(3 - \nu/2)}{\Gamma(\nu - 2)} \\ &\times [-\nu/2 - 2(\nu/2 - 2)^2].\end{aligned}\quad (\text{A45})$$

With the vertex function in hand, the virtual-gluon correction to the zeroth-order cross section can be evaluated easily. This interference contribution to the quark-antiquark squared amplitude

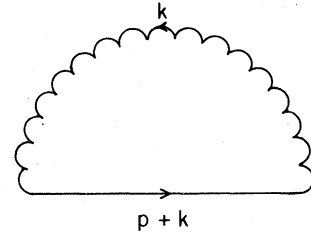


FIG. 9. Quark self-energy insertion giving the wave-function renormalization.

is given by [cf. Eq. (A6)]

$$\begin{aligned} |T_2|_{\text{virt}}^2 &= \frac{e^4 k^{8-2\nu}}{W^2} L_{\mu\nu} \\ &\times \sum_f 3Q_f^2 \text{tr} \gamma^\mu \gamma \cdot \bar{p} \gamma^\nu \gamma \cdot p \, 2 \text{Re}I(-W^2). \end{aligned} \quad (\text{A46})$$

Here the kinematics of the two-particle production requires that $2\vec{p} \cdot p = -W^2$ and $\vec{p} = -\vec{p}$. Calculating the trace and using Eq. (A7) for the perfectly po-

larized lepton tensor $L_{\mu\nu}$ gives

$$\begin{aligned} |T_2|_{\text{virt}}^2 &= 2e^4 k^{8-2\nu} \\ &\times \sum_f 3Q_f^2 [1 - (\hat{p} \cdot \hat{b})^2] 2 \text{Re}I(-W^2). \end{aligned} \quad (\text{A47})$$

We introduce this into the dimensionally continued double energy cross-section formula (A18) to compute the virtual-gluon exchange interference contribution. We find

$$\frac{d^2\Sigma^{(\text{virt})}}{d\Omega d\Omega'} = \frac{\alpha^2}{6W^2} \sum_f 3Q_f^2 \sin^2\psi [\delta^{(\nu-2)}(\Omega + \Omega') + \delta^{(\nu-2)}(\Omega - \Omega')] \frac{1}{2} \left(\frac{W}{4\pi k^2} \right)^{\nu-4} 2 \text{Re}I(-W^2), \quad (\text{A48})$$

where $\delta^{(\nu-2)}(\Omega + \Omega')$ denotes a solid-angle δ function for the anticollinear orientation and arises from detecting the quark and antiquark, while the collinear $\delta^{(\nu-2)}(\Omega - \Omega')$ arises from the "transparent" calorimeters detecting a quark or antiquark.

The total δ -function contribution in the collinear direction is obtained by summing Eqs. (A34) and (A48) to obtain the $\nu \rightarrow 4$ limit

$$\begin{aligned} \frac{d^2\Sigma^{(\text{col})}}{d\Omega d\Omega'} &= \frac{\alpha^2}{6W^2} \frac{\kappa^{12-3\nu} W^{2\nu-8}}{(4\pi)^{(3/2)\nu-6}} \sum_f 3Q_f^2 \frac{g^2}{4\pi^2} \\ &\times \delta^{(\nu-2)}(\Omega - \Omega') \left\{ \left[-\frac{3}{2(\nu/2-2)} + \left(-\frac{3}{2}\gamma + \frac{161}{24}\right) \right] \sin^2\psi + \frac{2}{3}(3\cos^2\psi - 1) \right\}, \end{aligned} \quad (\text{A49})$$

while the δ -function contribution in the anticollinear orientation is found from Eq. (A48) to be

$$\frac{d^2\Sigma^{(\text{anticol})}}{d\Omega d\Omega'} = \frac{\alpha^2}{6W^2} \frac{\kappa^{12-3\nu} W^{2\nu-8}}{(4\pi)^{(3/2)\nu-6}} \sum_f 3Q_f^2 \frac{g^2}{4\pi^2} \delta^{(\nu-2)}(\Omega + \Omega') \left[\frac{-2}{(\nu/2-2)^2} + \frac{(3-2\gamma)}{(\nu/2-2)} + (-\gamma^2 + 3\gamma - 8 + \frac{7}{6}\pi^2) \right] \sin^2\psi. \quad (\text{A50})$$

Using the δ functions, we can integrate these contributions over the small patches about the collinear and anticollinear orientations. Adding the integrated Eq. (A49) to Eq. (A33) gives the finite $\nu \rightarrow 4$ limit:

$$\int_{0 \leq \xi \leq \xi_0} d^{\nu-2}\Omega' \frac{d^2\Sigma}{d\Omega d\Omega'} = \frac{\alpha^2}{6W^2} \sum_f 3Q_f^2 \frac{g^2}{4\pi^2} \left[\left(\frac{3}{2}\ln\xi_0 + \frac{13}{24}\right) \sin^2\psi + \frac{2}{3}(3\cos^2\psi - 1) \right], \quad (\text{A51})$$

while summing Eq. (A32) and the integrated Eq. (A50) also yields a finite $\nu \rightarrow 4$ limit:

$$\int_{1-\xi_0 \leq \xi \leq 1} d^{\nu-2}\Omega' \frac{d^2\Sigma}{d\Omega d\Omega'} = \frac{\alpha^2}{6W^2} \sum_f 3Q_f^2 \frac{g^2}{4\pi^2} [-\ln^2\xi_0 - 3\ln\xi_0 - 4 - \pi^2/3] \sin^2\psi. \quad (\text{A52})$$

We see that the energy-energy angular correlation function is indeed finite in a distribution-theory sense.

As a final check, let us verify that the sum rule (A5) holds in order g^2 . Equations (A51) and (A52) give the integrals over small patches surrounding the integration end points. Thus we need only integrate over the intermediate range $\xi_0 \leq \xi \leq 1 - \xi_0$. In this region, the energy-energy cross section is everywhere finite so that we can set $\nu = 4$ in Eq. (A29), use the law of cosines to relate ψ' to ψ and χ [cf. Fig. 8], and secure the integral

$$\int_{\xi_0 \leq \xi \leq 1-\xi_0} d\Omega' \frac{d^2\Sigma}{d\Omega d\Omega'} = \frac{\alpha^2}{6W^2} \sum_f 3Q_f^2 \frac{g^2}{4\pi^2} \left\{ \left[\ln^2\xi_0 + \frac{3}{2}\ln\xi_0 + \frac{155}{24} + \frac{\pi^2}{3} \right] \sin^2\psi + \frac{7}{3}(3\cos^2\psi - 1) \right\}. \quad (\text{A53})$$

Adding this result to Eqs. (A51) and (A52), we note that the logarithms of the small angular cutoff ξ_0 cancel, as they must, and we find that

$$\int d\Omega' \frac{d^2\Sigma}{d\Omega d\Omega'} = \frac{\alpha^2}{2W^2} \sum_f 3Q_f^2 \frac{g^2}{4\pi^2} 2 \cos^2\psi. \quad (\text{A54})$$

This is identical to the $O(g^2)$ energy pattern, Eq. (1.7) (with $P=1$), verifying the sum rule.

APPENDIX B

The energy-energy cross section involving the production of quarks and gluons was calculated in Appendix A. However, in order to make connection with experiment, we need to estimate two additional effects. First of all, there are modifications of the perturbative QCD result caused by the fragmentation of quarks into the observed hadrons. Second, the semihadronic decay modes of heavy leptons contaminate the data. In this appendix, we shall analyze these two processes within a common framework which describes the fragmentation corrections to the members of the energy-cross-section hierarchy. The specific effects of the two types of fragmentation will then be evaluated using simple phenomenological models. Rough approximations will suffice for the heavy-lepton corrections since they are very small at high energy.

We begin by reviewing the effects of fragmentation upon the energy cross section $d\Sigma/d\Omega$. (A more complete discussion is found in Ref. 9.) The fragmentation of the parent (a quark or a heavy lepton) moving with momentum \vec{p} produces a number dn of hadrons in the momentum interval (d^3h) given by

$$dn = \frac{(d^3h)}{h^0} f_1(\vec{h}; \vec{p}). \quad (\text{B1})$$

This function obeys a sum rule expressing energy-momentum conservation,

$$\int \frac{(d^3h)}{h^0} h^\mu f_1(\vec{h}; \vec{p}) = p^\mu. \quad (\text{B2})$$

The fragmentation correction and the QCD effects are small at high energies. Hence, the fragmentation effect at high energy can be calculated by assuming that the parents of the hadrons are produced with the lowest-order two-body cross section $d\sigma/d\Omega_p$. The partial energy cross section with hadrons observed in a phase-space volume Δ is given by

$$\Delta\Sigma = \int d\Omega_p \frac{d\sigma}{d\Omega_p} \int_{\Delta} \frac{(d^3h)}{h^0} \left(\frac{h^0}{W}\right) [f_1(\vec{h}; \vec{p}) + f_1(\vec{h}; -\vec{p})]. \quad (\text{B3})$$

The two terms in the brackets of (B3) represent

the contribution from each of the two parents which are produced back to back in the laboratory frame. Extracting the solid-angle element $d\Omega$ of the detected energy from $(d^3h) = d\Omega h^2 dh$, we may express Eq. (B3) in the convenient form

$$\frac{d\Sigma}{d\Omega} = \frac{1}{2} \int d\Omega_p \frac{d\sigma}{d\Omega_p} [F_1(\eta) + F_1(\pi - \eta)], \quad (\text{B4})$$

where

$$F_1(\eta) = \frac{2}{W} \int h^2 dh f_1(\vec{h}; \vec{p}), \quad (\text{B5})$$

and η is the opening angle between the parent and the observed hadron, $\cos\eta = \hat{p} \cdot \hat{h}$. From the energy component of the sum rule (B2) we see that

$$\int d\Omega F_1(\eta) = 1, \quad (\text{B6})$$

and hence

$$\int d\Omega \frac{d\Sigma}{d\Omega} = \sigma_{\text{tot}}. \quad (\text{B7})$$

The general formula (B5) will now be applied to models representing the two types of fragmentation. First, we consider the fragmentation of a quark. Taking for convenience that the annihilating electrons and positrons are completely polarized, the lowest-order cross section is given by

$$\frac{d\sigma}{d\Omega_p} = \frac{\alpha^2}{2W^2} \sum_f 3Q_f^2 \sin^2\xi, \quad (\text{B8})$$

where ξ is the angle between the quark momentum \vec{p} and the beam polarization \hat{b} . Guided by experiment, we assume hadronic scaling so that the quark-fragmentation function depends only on h_\perp and $z = 2h_\parallel/W$, with h_\parallel and h_\perp the components of the hadronic momentum \vec{h} that are parallel and perpendicular to the quark momentum \vec{p} . Thus

$$f_1(\vec{h}; \vec{p}) = f_1(z, h_\perp). \quad (\text{B9})$$

We also assume that $f_1(z, h_\perp)$ decreases rapidly as the transverse momentum h_\perp increases, such that all moments of the h_\perp distribution exist, and that there is little backward production so that the scaling variable z may be limited to the range $0 < z < 1$. Hence the angular distribution $F_1(\eta)$ defined by Eq. (B6) vanishes in the backward hemisphere ($\eta > \pi/2$), and in the forward hemisphere ($\eta < \pi/2$) it is given by

$$F_1(\eta) = \frac{2}{W} \int h^2 dh f_1(z, h_\perp). \quad (\text{B10})$$

Making the simple change of variable $h = h_\perp/\sin\eta$, we have

$$F_1(\eta) = \frac{1}{\pi W} \sin^{-3}\eta \int (d^2h_\perp) h_\perp f_1\left(\frac{2}{W} h_\perp \cot\eta, h_\perp\right). \quad (\text{B11})$$

The high-energy behavior is nonuniform in the neighborhood of $\eta=0$, but for opening angles $\eta \gg \langle h_\perp \rangle / W$ we may set $z = (2/W) h_\perp \cot\eta = 0$ in $f_1(z, h_\perp)$ to obtain the limit as $W \rightarrow \infty$:

$$\begin{aligned} F_1(\eta) &\approx \frac{1}{\pi W} \sin^{-3}\eta \int (d^2h_\perp) h_\perp f_1(0, h_\perp) \\ &= \frac{C}{2\pi} \frac{\langle h_\perp \rangle}{W} \sin^{-3}\eta \quad (\eta < \pi/2). \end{aligned} \quad (\text{B12})$$

Here $\langle h_\perp \rangle$ is the transverse momentum defined by

$$\langle h_\perp \rangle = \frac{\int (d^2h_\perp) h_\perp f_1(0, h_\perp)}{\int (d^2h_\perp) f_1(0, h_\perp)} \quad (\text{B13})$$

and

$$C = 2 \int (d^2h_\perp) f_1(0, h_\perp) \quad (\text{B14})$$

is the coefficient of the logarithmic rise of the total hadronic multiplicity $\langle n \rangle_{\text{tot}}$ in e^+e^- annihilation,

$$\langle n \rangle_{\text{tot}} = C \ln W + \text{constant}. \quad (\text{B15})$$

Therefore, $F_1(\eta)$ is small (proportional to $1/W$) for all values of η which are not within the peak at $\eta=0$. The height of this peak is given by

$$\begin{aligned} F_1(0) &= \frac{2}{W} \int h^2 dh f_1\left(\frac{2}{W} h, 0\right) \\ &= \frac{W^2}{4} \int_0^1 z^2 dz f_1(z, 0), \end{aligned} \quad (\text{B16})$$

increasing as W^2 with a coefficient that cannot be determined in a model-independent way. Since Eq. (B6) requires that the distribution $F_1(\eta)$ integrated over $2\pi \sin\eta d\eta$ give unity, the width of this peak is of order $1/W$. Thus the angular dependence of $F_1(\eta)$ must show the general behavior illustrated in Fig. 10. We can now exploit these properties to evaluate the energy cross section (B4). We use the laws of cosines to write the $\sin^2\xi$ appearing in (B8) in terms of the jet opening angle η and the angle ψ between \hat{h} and $\hat{\delta}$ and average over an azimuthal angle to secure the replacement

$$\sin^2\xi \rightarrow \sin^2\psi + \frac{1}{2}\sin^2\eta(3\cos^2\psi - 1), \quad (\text{B17})$$

and hence

$$\begin{aligned} \frac{d\Sigma}{d\Omega} &= \frac{\alpha^2}{4W^2} \sum_f 3Q_f^2 \int d\Omega_p [\sin^2\psi + \frac{1}{2}\sin^2\eta(3\cos^2\psi - 1)] \\ &\quad \times [F_1(\eta) + F_1(\pi - \eta)]. \end{aligned} \quad (\text{B18})$$

Since the integrand now depends only on $\vec{p} \cdot \vec{h}$ we

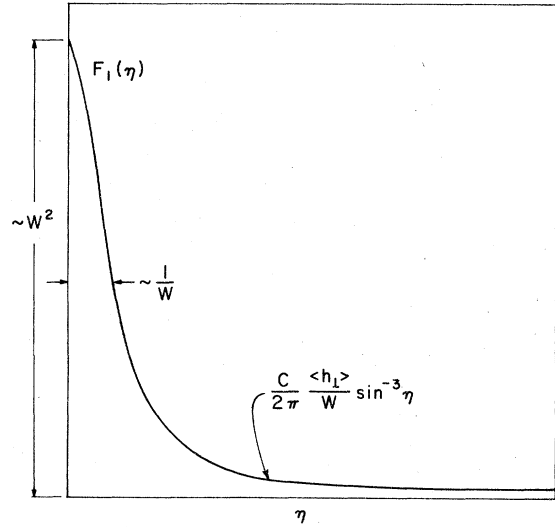


FIG. 10. Schematic illustration of the hadronic angular distribution $F_1(\eta)$ in the fragmentation of a high-energy quark.

may consider $d\Omega_p$ to be a solid-angle element of the hadronic momentum \vec{h} rather than that of the quark momentum \vec{p} . Then, by using the normalization condition (B6), we can write

$$\frac{d\Sigma}{d\Omega} = \frac{\alpha^2}{2W^2} \sum_f 3Q_f^2 [\sin^2\psi + \frac{1}{2}\langle \sin^2\eta \rangle^{(qt)} (3\cos^2\psi - 1)], \quad (\text{B19})$$

where

$$\langle \sin^2\eta \rangle^{(qt)} = \int_{\eta < \pi/2} d\Omega \sin^2\eta F_1(\eta) \quad (\text{B20})$$

defines an energy-weighted average opening angle. Since this average is insensitive to the structure of $F_1(\eta)$ for small values of η , we may use the leading form (B12) to obtain

$$\langle \sin^2\eta \rangle^{(qt)} = \frac{\pi C}{2} \frac{\langle h_\perp \rangle}{W}. \quad (\text{B21})$$

We can analyze the smearing of the energy pattern caused by the fragmentation of heavy leptons into hadrons with a parallel procedure. The lowest-order cross section for the production of heavy leptons (which eventually form hadronic systems accompanied by undetected neutrinos) is given by

$$\begin{aligned} \frac{d\sigma}{d\Omega_p} &= \beta^2 \left(\frac{\alpha^2}{2W^2} \right) \left(1 - \frac{4M^2}{W^2} \right)^{1/2} \\ &\quad \times \left[\left(1 + \frac{2M^2}{W^2} \right) \sin^2\xi + \frac{2M^2}{W^2} (3\cos^2\xi - 1) \right], \end{aligned} \quad (\text{B22})$$

where M is the lepton mass and ξ is now the angle between the lepton momentum \vec{p} and the polariza-

tion axis \hat{b} . We have included factors of the semi-hadronic branching ratio β for the heavy lepton since the purely leptonic decays can be excluded from the data. We shall account for the fact that the undetected neutrinos carry away on average a fraction $1 - \gamma$ of the energy by multiplying our final result by a factor γ . We construct the fragmentation model in this case from the assumption that the decay distribution of the heavy lepton is spherically symmetric in its rest frame. The lepton fragmentation function is thus given by a simple phase-space model which depends only upon the Lorentz scalar $-(p-h)^2$,

$$f_1(\vec{h}; \vec{p}) = f_1[-(p-h)^2], \quad (\text{B23})$$

yielding, when inserted in (B5), an angular distribution

$$F_1(\eta) = \frac{2}{W} \int h^2 dh f_1[-(p-h)^2]. \quad (\text{B24})$$

We shall assume that the mass of the produced hadrons can be neglected and take $h^0 = h$. This should induce little error since most of these hadrons are pions. The kinematical constraints $-(p-h)^2 > 0$ and $(p-h)^0 > 0$ are tantamount to the restriction $0 < h < h_{\max}(\eta)$ where, with $p^0 = W/2$,

$$\frac{d\Sigma}{d\Omega} = \beta^2 \gamma \left(\frac{\alpha^2}{2W^2} \right) \left(1 - \frac{4M^2}{W^2} \right)^{1/2} \left\{ \left(1 + \frac{2M^2}{W^2} \right) \sin^2 \psi + \frac{1}{2} \left[\langle \sin^2 \eta \rangle + \frac{4M^2}{W^2} \langle \cos^2 \eta \rangle \right] (3 \cos^2 \psi - 1) \right\}. \quad (\text{B30})$$

The energy-weighted averages can easily be computed using (B29). In the high-energy limit

$$\langle \sin^2 \eta \rangle \simeq 4M^2/W^2 \quad (\text{B31})$$

and

$$\frac{d\Sigma}{d\Omega} \simeq \beta^2 \gamma \left(\frac{\alpha^2}{2W^2} \right) \left[\sin^2 \psi + \frac{4M^2}{W^2} (3 \cos^2 \psi - 1) \right]. \quad (\text{B32})$$

We now turn to the evaluation of fragmentation effects for the next member of our hierarchy, the energy-energy cross section. Since this quantity involves a two-hadron distribution, we must introduce another function $f_2(\vec{h}, \vec{h}'; \vec{p})$ which gives the

$$\frac{d^2\Sigma}{d\Omega d\Omega'} = \int d\Omega_p \frac{d\sigma}{d\Omega_p} \int \frac{h^2 dh}{h^0} \frac{h'^2 dh'}{h'^0} \left(\frac{h^0}{W} \right) \left(\frac{h'^0}{W} \right) \times \{ [f_1(\vec{h}; \vec{p}) f_1(\vec{h}'; -\vec{p}) + f_2(\vec{h}, \vec{h}'; \vec{p}) + h^0 \delta(\vec{h} - \vec{h}') f_1(\vec{h}; \vec{p})] + [\vec{p} \leftrightarrow -\vec{p}] \}. \quad (\text{B35})$$

The first two terms within the brackets correspond to the cases where the hadrons arise from the fragmentation of distinct parents and from the same parent. The third term within the brackets is a consequence of our prescription dealing with coincident detection. It is easy to verify from the energy component of the sum rules (B2) and (B34) that Eq. (B35) obeys the normalization

$$h_{\max}(\eta) = \frac{M^2}{W} (1 - v \cos \eta)^{-1}, \quad (\text{B25})$$

and $v = p/p^0$ is the velocity of the heavy lepton. Thus, introducing the variable

$$x = \frac{h}{h_{\max}(\eta)} = \frac{hW}{M^2} (1 - v \cos \eta), \quad (\text{B26})$$

which has the kinematic limits $0 \leq x \leq 1$, we can write

$$-(p-h)^2 = M^2(1-x) \quad (\text{B27})$$

and obtain

$$F_1(\eta) = \frac{2M^6}{W^4} \frac{1}{(1-v \cos \eta)^3} \int_0^1 x^2 f_1[M^2(1-x)] dx. \quad (\text{B28})$$

The value of the integral can be obtained from the normalization condition (B6), yielding the result

$$F_1(\eta) = \frac{4}{\pi} \left(\frac{M}{W} \right)^4 \frac{1}{[1 - v \cos \eta]^3}. \quad (\text{B29})$$

Equations (B4), (B22), and the law of cosines now give, including the factor γ for the fraction of the energy carried off by the detected hadrons,

average number of hadron pairs d^2n produced in the momentum interval $(d^3h)(d^3h')$ from the fragmentation of a parent with momentum \vec{p} ,

$$d^2n = \frac{(d^3h)}{h^0} \frac{(d^3h')}{h'^0} f_2(\vec{h}, \vec{h}'; \vec{p}). \quad (\text{B33})$$

Energy-momentum conservation imposes the constraints²²

$$\int \frac{(d^3h')}{h'^0} h'^{\mu} f_2(\vec{h}, \vec{h}'; \vec{p}) = (p^{\mu} - h^{\mu}) f_1(\vec{h}; \vec{p}). \quad (\text{B34})$$

A general expression for the energy-energy cross section in terms of the fragmentation functions may be written in a manner similar to that used for the energy cross section:

$$\int \frac{d^2\Sigma}{d\Omega d\Omega'} d\Omega' = \frac{d\Sigma}{d\Omega}. \quad (\text{B36})$$

As before, it is convenient to express Eq. (B35) in the form

$$\frac{d^2\Sigma}{d\Omega d\Omega'} = \frac{1}{4} \int d\Omega_p \frac{d\sigma}{d\Omega_p} [F_1(\eta)F_1(\pi - \eta') + F_1(\pi - \eta)F_1(\eta') + F_2(\eta, \eta', \chi) + F_2(\pi - \eta, \pi - \eta', \chi)], \quad (\text{B37})$$

where we have used (B5) and defined

$$F_2(\eta, \eta', \chi) = \left(\frac{2}{W}\right)^2 \int h^2 dh h'^2 dh' [f_2(\vec{h}, \vec{h}'; \vec{p}) + h^0 \delta(\vec{h} - \vec{h}') f_1(\vec{h}; \vec{p})]. \quad (\text{B38})$$

Here η and η' are the two opening angles defined by $\cos\eta = \hat{p} \cdot \hat{h}$, $\cos\eta' = \hat{p} \cdot \hat{h}'$, and χ is the angle between the hadronic momenta, $\cos\chi = \hat{h} \cdot \hat{h}'$. It follows from the sum rule (B34) that

$$\int d\Omega' F_2(\eta, \eta', \chi) = F_1(\eta). \quad (\text{B39})$$

Assuming scaling, the two-particle function for the fragmentation of a quark can depend only on the variables $z = 2h_{||}/W$, $z' = 2h'_{||}/W$ and $\vec{h}_\perp, \vec{h}'_\perp$:

$$f_2(\vec{h}, \vec{h}'; \vec{p}) = f_2(z, \vec{h}_\perp; z', \vec{h}'_\perp). \quad (\text{B40})$$

The general features of the double angular distribution F_2 can be deduced by using methods similar to those employed in the analysis of the single angular distribution F_1 . Thus, by changing integration variables in (B38) from h and h' to $h_{||}/\sin\eta$ and $h'_{||}/\sin\eta'$, we find that when both opening angles η and η' are large compared to $1/W$, $F_2(\eta, \eta'; \chi)$ is proportional to $1/W^2$ in the high-energy limit. However, we cannot determine the coefficient of this energy factor for the two-particle fragmentation in a model-independent way as was done for the single-particle function [Eq. (B12)]. Although F_2 is quite small in this angular region (of order W^{-2}), it is strongly peaked when either of the two opening angles becomes very small. This peaking is required by the normalization (B39) since $F_1(\eta)$ is of order W^{-1} .

Armed with these facts, we can now extract the leading contribution to the energy-energy cross section from quark fragmentation. We observe that evaluating the integral over the solid angle Ω_p in (B37) yields nonleading contributions as $W \rightarrow \infty$ except for small angular regions about directions which are aligned either collinearly or anticollinearly with a detection direction Ω or Ω' . These are regions where the value of an opening angle approaches 0 or π with the integration including a fragmentation peak. (We shall constrain the angle χ between the two detectors to be away from 0 or π . If $\chi = 0$ or π , the interaction would run simultaneously over peaks for both opening angles.) As an example, consider the contribution which comes from integrating over the patch about

$\Omega_p \simeq \Omega$ which implies that $\eta \simeq 0$ and $\eta' \simeq \chi$. Here the angular distributions $F_1(\eta)$ and $F_2(\eta, \eta', \chi)$ are rapidly varying in η . We can expand the dependence of the rest of the integrand on the variables Ω_p and η' as power series in the small opening angle η for fixed χ ; the dominant pieces are obtained from the zeroth-order term of this series. Hence, the integral is evaluated over this region by taking $d\Omega_p \simeq d\Omega$, $d\sigma/d\Omega_p \simeq d\sigma/d\Omega$, and $\eta' \simeq \chi$, yielding the contribution

$$\frac{1}{4} \frac{d\sigma}{d\Omega} \left[F_1(\pi - \chi) \int d\Omega F_1(\eta) + \int d\Omega F_2(\eta, \chi, \chi) \right]. \quad (\text{B41})$$

The values of the integrals appearing here are determined from the normalization constraints (B6) and (B39). That they do not extend over the full solid angle is of no consequence since the leading terms in both cases are obtained from small angular regions. Thus, the result of the integration over the patch about $\Omega_p \simeq \Omega$ is

$$\frac{1}{4} \frac{d\sigma}{d\Omega} \{F_1(\pi - \chi) + F_1(\chi)\}. \quad (\text{B42})$$

The inclusion of all such regions in Eq. (B37) yields

$$\frac{d^2\Sigma}{d\Omega d\Omega'} \simeq \frac{1}{2} [F_1(\chi) + F_1(\pi - \chi)] \left(\frac{d\sigma}{d\Omega} + \frac{d\sigma}{d\Omega'} \right). \quad (\text{B43})$$

Using the distribution function F_1 given in Eq. (B12) for $\chi < \pi/2$ and noting that, since $\sin(\pi - \chi) = \sin\chi$ the contributions to the forward and backward hemispheres are identical in form, we find ($0 < \chi < \pi$)

$$\frac{d^2\Sigma}{d\Omega d\Omega'} \simeq \frac{C}{4\pi} \frac{\langle h_{||} \rangle}{W} \sin^{-3}\chi \left(\frac{d\sigma}{d\Omega} + \frac{d\sigma}{d\Omega'} \right). \quad (\text{B44})$$

We shall show later, after some travail, that the corrections to this formula are of order $1/W^2$.

The forms (B43) and (B44) for the fragmentation effect on the energy-energy cross section are, as remarked above, not valid for $\chi \sim 0$ or $\chi \sim \pi$. In particular, they do not obey the normalization condition (B36). However, we may use these forms to evaluate a moment such as $\langle \sin^2\chi \rangle$ which

involves a function that vanishes sufficiently rapidly at $\chi=0$ and $\chi=\pi$ to ensure that the contributions of the integration range with $\sin\chi \ll \langle h \rangle/W$ are negligible. In order to emphasize the symmetry of the fragmentation effects, we consider separate averages of $\sin^2\chi$ in the forward ($\chi < \pi/2$) and backward ($\chi > \pi/2$) hemispheres, defining

$$\langle \sin^2\chi \rangle_F = \frac{1}{\sigma_{\text{tot}}} \int_{\chi < \pi/2} d\Omega d\Omega' \sin^2\chi \frac{d^2\Sigma}{d\Omega d\Omega'} \quad (\text{B45a})$$

and

$$\langle \sin^2\chi \rangle_B = \frac{1}{\sigma_{\text{tot}}} \int_{\chi > \pi/2} d\Omega d\Omega' \sin^2\chi \frac{d^2\Sigma}{d\Omega d\Omega'}. \quad (\text{B45b})$$

Using Eq. (B43), we find that to leading order

$$\begin{aligned} \langle \sin^2\chi \rangle_F &= \int d\Omega' \sin^2\chi F_1(\chi) \frac{1}{\sigma_{\text{tot}}} \int d\Omega \frac{d\Sigma}{d\Omega} \\ &= \langle \sin^2\eta \rangle \\ &= \langle \sin^2\chi \rangle_B. \end{aligned} \quad (\text{B46})$$

The forward and backward averages of this measure of the angle between the two energy detectors are thus identical in leading order and equal to the measure of the average jet opening angle defined in Eq. (B20). This is in sharp contrast with the QCD behavior.

A parallel treatment of the contribution of the semihadronic decays of a heavy lepton to the energy-energy cross section is hampered by the fact that energy is carried off by neutrinos which are not detected. The heavy-lepton contribution is, however, roughly similar to that made by quark fragmentation except that, on average, a fraction $(1-\gamma)$ of the energy is carried off by neutrinos and not detected. Since the heavy-lepton effects are very small, this rough similarity provides a sufficiently accurate estimate. Hence we may use the angular distribution (B29) in the general formula (B43) along with an additional factor of γ^2 to get

$$\begin{aligned} \frac{d^2\Sigma}{d\Omega d\Omega'} &\simeq \frac{2\gamma^2}{\pi} \left(\frac{M}{W}\right)^4 \left[\frac{1}{(1-v\cos\chi)^3} + \frac{1}{(1+v\cos\chi)^3} \right] \\ &\times \left(\frac{d\sigma}{d\Omega} + \frac{d\sigma}{d\Omega'} \right), \end{aligned} \quad (\text{B47})$$

with the heavy-lepton production cross section $d\sigma/d\Omega'$ being given by Eq. (B22).

We have found that, for detectors which are not collinear ($\chi \approx 0$) or anticollinear ($\chi \approx \pi$), the leading contribution is of order $1/W$ and arises from uncorrelated quark fragmentation while the heavy-lepton contribution is negligible, of order $1/W^4$. Conceivably, there could be quark-fragmentation contribution of, say, order $\ln W/W^2$. We turn now to show that, this is not the case but that,

with $\chi \neq 0$, the quark-fragmentation contribution to the energy-energy cross section may be expressed entirely in terms of the single-hadron distribution F_1 plus a remainder which is of order $1/W^2$. To do this, we introduce a two-particle correlation function $c(\vec{h}, \vec{h}'; \vec{p})$ by writing

$$f_2(\vec{h}, \vec{h}'; \vec{p}) = f_1(\vec{h}; \vec{p}) f_1(\vec{h}'; \vec{p}) + c(\vec{h}, \vec{h}'; \vec{p}). \quad (\text{B48})$$

The energy-momentum sum rules (B2) and (B34) and the decomposition (B48) of f_2 into uncorrelated and correlated pieces give

$$\int \frac{(d^3h')}{h'^0} h'^\mu c(\vec{h}, \vec{h}'; \vec{p}) = -h^\mu f_1(\vec{h}; \vec{p}). \quad (\text{B49})$$

Assuming that the detectors are not coincident, we may insert the decomposition (B48) into the general fragmentation formula (B35) for the energy-energy cross section to get

$$\begin{aligned} \frac{d^2\Sigma}{d\Omega d\Omega'} &= \frac{1}{4} \int d\Omega_p \frac{d\sigma}{d\Omega_p} [F_1(\eta) + F_1(\pi - \eta)] \\ &\times [F_1(\eta') + F_1(\pi - \eta')] + R + \bar{R}, \end{aligned} \quad (\text{B50})$$

where R (\bar{R}) describes the correlated fragmentation of the quark (antiquark),

$$R = \frac{1}{W^2} \int d\Omega_p \frac{d\sigma}{d\Omega_p} \int h^2 dh h'^2 dh' c(\vec{h}, \vec{h}'; \vec{p}), \quad (\text{B51})$$

with \bar{R} given by an entirely similar expression save for \vec{p} being replaced by $\vec{p} = -\vec{p}$. We shall now prove that if the detectors are not collinear ($\chi \sim 0$), then R (and hence also \bar{R}) is of order $1/W^2$. Thus, with $\chi \neq 0$ and to order $1/W^2$, R and \bar{R} can be neglected in Eq. (B50) and the quark-fragmentation contribution to the energy-energy cross section is expressed in terms of the single-particle distributions F_1 .

With the scaling hypothesis, the correlation function c depends only upon $h_1, h'_1, \vec{h}_1 \cdot \vec{h}'_1$, $z = 2h_{\parallel}/W$, and $z' = 2h'_{\parallel}/W$. Recalling that the angles between \vec{h} , \vec{h}' , and \vec{p} are denoted by η, η' , we have

$$h = h_1/\sin\eta, \quad h' = h'_1/\sin\eta', \quad (\text{B52})$$

and

$$z = \frac{2h_1}{W} \cot\eta, \quad z' = \frac{2h'_1}{W} \cot\eta'. \quad (\text{B53})$$

Choosing h_1 and h'_1 as the integration variables gives

$$\begin{aligned} R &= \frac{1}{W^2} \int d\Omega_p \frac{d\sigma}{d\Omega_p} \int \frac{h_1^2 dh_1 h'^2 dh'_1}{\sin^3\eta \sin^3\eta'} \\ &\times c(h_1, h'_1, \vec{h}_1 \cdot \vec{h}'_1, z, z'). \end{aligned} \quad (\text{B54})$$

The h_1 and h'_1 integrations are effectively bounded

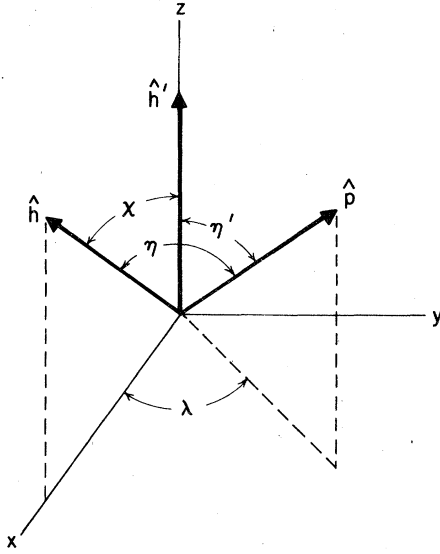


FIG. 11. Coordinate system used to specify the direction of the quark momentum \hat{p} relative to the plane of the hadron momenta in terms of the angles η' and λ .

by the cutoffs in the correlation function c . Hence Eq. (B54) is of the order $1/W^2$ displayed by the first factor except possibly for integration regions where η or η' become very small. Since $\chi \neq 0$, η and η' cannot both be small simultaneously. Since there is a complete symmetry between η and η' , it suffices to consider the case when η' is small. Let us initially set up a coordinate system with \hat{h}' lying along the z axis and \hat{h} lying in the x - z plane as shown in Fig. 11. The quark direction \hat{p} is now specified by a polar angle η' and an azimuthal angle λ , with

$$d\Omega_p = d\lambda \sin\eta' d\eta'. \quad (\text{B55})$$

We see that the integral in Eq. (B54) involves a factor $(\sin\eta')^{-2}$ which might give large contributions counterbalancing the first $1/W^2$ factor.

To investigate this possibility, we can expand the remainder of the integrand in powers of $\sin\eta'$. Only terms of zeroth and first order in $\sin\eta'$ give rise to potentially large contributions so that we need only examine these terms. We must except, of course, $z' = (2h'_1/W) \cot\eta'$ from this expansion. To first order in $\sin\eta'$,

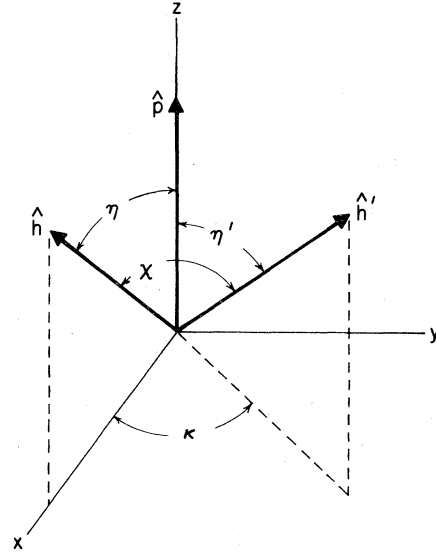


FIG. 12. Coordinate system which defines the new azimuthal angle κ .

$$\vec{h}_1 \cdot \vec{h}'_1 = -h_1 h'_1 (\cos\lambda - \sin\eta' \sin^2\lambda \cot\chi), \quad (\text{B56})$$

where χ is the angle between \vec{h} and \vec{h}' . It will prove convenient to refer to a new coordinate system where \hat{p} is taken to lie along the z axis with \vec{h} lying in the x - z plane as illustrated in Fig. 12. Now the orientation of \vec{h}' is described by the polar angle η' and by an azimuthal angle κ . In terms of this new azimuthal angle we have simply

$$\vec{h}_1 \cdot \vec{h}'_1 = h_1 h'_1 \cos\kappa \quad (\text{B57})$$

and, on comparing with Eq. (B56), to first order in $\sin\eta'$,

$$\cos\lambda \approx -\cos\kappa + \sin\eta' \sin^2\kappa \cot\chi \quad (\text{B58})$$

and

$$d\lambda \approx d\kappa (1 + \sin\eta' \cos\kappa \cot\chi). \quad (\text{B59})$$

Moreover, to first order in $\sin\eta'$,

$$\sin\eta \approx \sin\chi + \sin\eta' \cos\chi \cos\kappa \quad (\text{B60})$$

and

$$\cot\eta \approx \cot\chi - \sin\eta' \cos\kappa (\sin\chi)^{-2}. \quad (\text{B61})$$

Therefore, the potentially large terms involving $(\sin\eta')^{-2}$ and $(\sin\eta')^{-1}$ are contained in

$$R_{\text{sing}} = \frac{1}{W^2} \frac{1}{\sin^3\chi} \int d\kappa \frac{d\eta'}{\sin^2\eta'} \frac{d\sigma}{d\Omega_p} \int h_1^2 dh_1 h_1'^2 dh_1' \left[1 + \sin\eta' \cos\kappa \left(\frac{\partial}{\partial\chi} - 2 \cot\chi \right) \right] \times c \left(h_1, h_1', h_1 h_1' \cos\kappa, \frac{2h_1}{W} \cot\chi, \frac{2h_1'}{W} \cot\eta' \right). \quad (\text{B62})$$

Here the quark production cross section $d\sigma/d\Omega_p$ should also be expanded about $\hat{p} = \hat{h}'$, keeping zeroth- and first-order terms in $\sin\eta'$. The only facet of this expansion that we need is the fact that terms linear in

$\sin\eta'$ correspond to small deviations of \hat{p} from \hat{h}' that lie in the x - y plane of Fig. 12. Hence, a term linear in $\sin\eta'$ must be accompanied by a single factor of $\cos\lambda \approx -\cos\kappa$ or $\sin\lambda \approx -\sin\kappa$. Accordingly, the potentially large pieces depend upon integrals of the type

$$\int d\kappa \int \frac{d\eta'}{\sin^2\eta'} \int h_{\perp}'^2 dh_{\perp}' \left\{ \begin{array}{c} 1 \\ \sin\eta' \cos\kappa \\ \sin\eta' \sin\kappa \end{array} \right\} c\left(h_{\perp}, h_{\perp}', h_{\perp} h_{\perp}' \cos\kappa, \frac{2h_{\perp}}{W} \cot\chi, \frac{2h_{\perp}'}{W} \cot\eta'\right). \quad (\text{B63})$$

All of these integrals are, however, controlled by the four-momentum sum rule (B49). Since small $\sin\eta'$ corresponds to large h' , we may neglect the mass of the produced hadron and take $h^0 = h$. Evaluating the $\mu = 0$, $\mu = x$, and $\mu = y$ components of the sum rule (B49) in the coordinate system of Fig. 12 gives

$$\int d\kappa \int \frac{d\eta'}{\sin^2\eta'} \int h_{\perp}'^2 dh_{\perp}' \left\{ \begin{array}{c} 1 \\ \sin\eta' \cos\kappa \\ \sin\eta' \sin\kappa \end{array} \right\} c\left(h_{\perp}, h_{\perp}', h_{\perp} h_{\perp}' \cos\kappa, \frac{2h_{\perp}}{W} \cot\eta, \frac{2h_{\perp}'}{W} \cot\eta'\right) \\ = -h_{\perp} \left\{ \begin{array}{c} 1/\sin\eta \\ 1 \\ 0 \end{array} \right\} f_1\left(\frac{2h_{\perp}}{W} \cot\eta, h_{\perp}\right). \quad (\text{B64})$$

Replacing η by χ , we see that all of the integrals in Eq. (B63) may be expressed in terms of $h_{\perp} f_1((2h_{\perp}/W)\cot\chi, h_{\perp})$ and hence Eq. (B62) has the form

$$R_{\text{sing}} \sim \frac{1}{W^2} \int h_{\perp}^3 dh_{\perp} f_1 \sim \frac{1}{W^2}. \quad (\text{B65})$$

Thus we have proved that R and \bar{R} are indeed of order $1/W^2$ if $\chi \neq 0$.

With the neglect of the order $1/W^2$ correlated fragmentation corrections, Eq. (B50) can be written as

$$\frac{d^2\Sigma}{d\Omega d\Omega'} \approx \frac{1}{4} \int d\Omega_p \frac{d\sigma}{d\Omega_p} [F_1(\eta) + F_1(\pi - \eta)][F_1(\eta') + F_1(\pi - \eta')]. \quad (\text{B66})$$

We shall now use this result to refine the arguments leading to the formula (B44) and prove that it is indeed accurate to order $1/W^2$. Since $F_1(\eta)$ is of order $1/W$ unless η is small, the angular integration in Eqs. (B66) gives terms of order $1/W^2$ except for regions where the argument of one of the F_1 functions is small. Let us consider, for example, the region where $0 \leq \eta \leq \epsilon$ with $\epsilon \ll 1$. Except for the factor of $F_1(\eta)$, the remainder of the integrand is of order $1/W$, and it is well behaved as a function of η . Let us denote this remaining factor by $W^{-1}G(\hat{p})$ so that we are investigating integrals of the type

$$I = \frac{1}{W} \int_{0 \leq \eta \leq \epsilon} d\Omega_p F_1(\eta) G(\hat{p}). \quad (\text{B67})$$

We use the spherical coordinates

$$\begin{aligned} \hat{p}_z &= \cos\eta, \\ \hat{p}_x &= \sin\eta \cos\phi, \quad \hat{p}_y = \sin\eta \sin\phi \end{aligned} \quad (\text{B68})$$

with

$$d\Omega_p = \sin\eta d\eta d\phi. \quad (\text{B69})$$

Since F_1 does not involve the azimuthal angle ϕ , the ϕ integration produces

$$\bar{G} = \frac{1}{2\pi} \int_0^{2\pi} d\phi G(\hat{p}). \quad (\text{B70})$$

This integration removes odd powers of $\sin\eta$ from \bar{G} since, according to Eq. (B68), these odd powers of $\sin\eta$ are associated with odd powers of $\cos\phi$ or $\sin\phi$. Moreover, $\cos\eta$ is an analytic function of $\sin^2\eta$ for small η . Hence we may write

$$\bar{G} = G(0) + \sin^2\eta \bar{G}_1(\sin^2\eta), \quad (\text{B71})$$

where $G(0)$ is the value of $G(\hat{p})$ when \hat{p} is aligned with \hat{h} . This decomposition gives

$$\begin{aligned} I &= \frac{1}{W} G(0) \int_{0 \leq \eta \leq \epsilon} d\Omega_p F_1(\eta) \\ &+ \frac{2\pi}{W} \int_0^{\epsilon} d\eta \sin^3\eta F_1(\eta) \bar{G}_1(\sin^2\eta). \end{aligned} \quad (\text{B72})$$

Since $F_1(\eta)$ is of order $1/W$ for $\eta > \epsilon$, the sum rule (B6) evaluates the first integral above,

$$\int_{0 \leq \eta \leq \epsilon} d\Omega_p F_1(\eta) = 1 + O(1/W). \quad (\text{B73})$$

To evaluate the second integral of Eq. (B72), we use the variable $h_1 = h \sin \eta$ in Eq. (B5) to secure

$$\begin{aligned} & \frac{2\pi}{W} \int_0^\epsilon d\eta \sin^3 \eta F_1(\eta) \bar{G}_1(\sin^2 \eta) \\ &= \frac{4\pi}{W^2} \int_0^\epsilon d\eta \int h_1^2 dh_1 f_1 \left(\frac{2h_1}{W} \cot \eta, h_1 \right) \bar{G}_1(\sin^2 \eta). \end{aligned} \quad (\text{B74})$$

The integration over h_1 is finite in the limit $W \rightarrow \infty$. Hence, Eq. (B74) is of order $1/W^2$ and we have proved that

$$I = \frac{1}{W} G(0) + O(1/W^2). \quad (\text{B75})$$

Using this result for all the regions where the arguments of the F_1 functions in Eq. (B66) become small, we get

$$\begin{aligned} \frac{d^2 \Sigma}{d\Omega d\Omega'} &= \frac{1}{2} [F_1(\chi) + F_1(\pi - \chi)] \left(\frac{d\sigma}{d\Omega} + \frac{d\sigma}{d\Omega'} \right) \\ &+ O(1/W^2), \end{aligned} \quad (\text{B76})$$

which proves that Eq. (B43) and hence Eq. (B44) are accurate to order $1/W^2$.

¹The theory is reviewed in W. Marciano and H. Pagels, *Phys. Rep.* **36**, 137 (1978).

²A. Belavin, A. Polyakov, A. Schwartz, and Y. Tyupkin, *Phys. Lett.* **59B**, 85 (1975); G. 't Hooft, *Phys. Rev. D* **14**, 3432 (1975); C. Callan, R. Dashen, and D. Gross, *Phys. Lett.* **63B**, 334 (1976); *Phys. Rev. D* **17**, 2717 (1978); R. Jackiw and C. Rebbi, *Phys. Rev. Lett.* **37**, 172 (1976). A review appears in S. Coleman, lectures at 1977 Ettore Majorana Summer School, Harvard report (unpublished).

³Renormalization-group techniques are described in *Methods in Field Theory*, edited by R. Balian and J. Zinn-Justin (North-Holland, Amsterdam, 1976).

⁴D. Gross and F. Wilczek, *Phys. Rev. Lett.* **30**, 1343 (1973); H. D. Politzer, *ibid.* **30**, 1346 (1973).

⁵T. Appelquist and H. Georgi, *Phys. Rev. D* **8**, 4000 (1973); A. Zee, *ibid.* **8**, 4038 (1973).

⁶See, e.g., A. De Rújula, H. Georgi, and H. D. Politzer, *Ann. Phys. (N.Y.)* **103**, 315 (1977).

⁷See, e.g., the reviews by K. Schultze, L. N. Hand, and O. Nachtman, in the *Proceedings of the 1977 International Symposium on Lepton and Photon Interactions at High Energies, Hamburg, Germany*, edited by F. Gutbrod (DESY, Hamburg, 1977).

⁸G. Sterman and S. Weinberg, *Phys. Rev. Lett.* **39**, 1436 (1977).

⁹C. L. Basham, L. S. Brown, S. D. Ellis, and S. T. Love, *Phys. Rev. D* **17**, 2298 (1978).

¹⁰Some work in arbitrary order in perturbation theory has been done by G. Sterman, *Phys. Rev. D* **17**, 2789 (1978) and G. Tiktopoulos, *Nucl. Phys.* **B147**, 371 (1979).

^{11(a)}H. Georgi and M. Machacek, *Phys. Rev. Lett.* **39**, 1237 (1977); E. Farhi, *ibid.* **39**, 1587 (1977); A. De Rújula, J. Ellis, E. G. Floratos, and M. K. Gaillard, *Nucl. Phys.* **B138**, 387 (1978); S.-S. Shei, *Phys. Lett.* **79B**, 245 (1978); S.-Y. Pi, R. Jaffe, and F. Low, *Phys. Rev. Lett.* **41**, 142 (1978).

^{11(b)}G. C. Fox and S. Wolfram, *Phys. Rev. Lett.* **41**, 1581 (1978) and CalTech Report No. CALT 68-680 (unpublished).

¹²These values are from the lecture of R. F. Schwitters, in *Proceedings of the 1975 International Symposium on Lepton Interactions at High Energies, Stanford, California*, edited by W. T. Kirk (SLAC, Stanford, 1975), p. 10, except that C is obtained by multiplying the charge multiplicity by $\frac{5}{3}$ rather than by the naive factor of $\frac{1}{3}$ in order to account roughly for the experimental observation that more than their share of the energy is carried off by neutral particles.

¹³M. L. Perl *et al.*, *Phys. Rev. Lett.* **35**, 1489 (1975); M. L. Perl *et al.*, *Phys. Lett.* **63B**, 466 (1976). A review appears in G. J. Feldman and M. L. Perl, *Phys. Rep.* **33C**, 285 (1977).

¹⁴The values for the mass M and branching fraction β are obtained from the review by G. J. Feldman, in *Neutrinos-78*, proceedings of the International Conference on Neutrino Physics and Astrophysics, Purdue Univ., edited by Earle C. Fowler (Purdue Univ., Lafayette, Indiana, 1978), p. 647. The value for γ was calculated for the standard model in which the τ decays into a massless neutrino ν_τ and a massless quark pair, assuming $V-A$ weak couplings.

¹⁵The double energy cross section was introduced in our earlier note, C. L. Basham, L. S. Brown, S. D. Ellis, and S. T. Love, *Phys. Rev. Lett.* **41**, 1585 (1978).

¹⁶C. L. Basham, L. S. Brown, S. D. Ellis, and S. T. Love (manuscript in preparation).

¹⁷Some discussion of a particular experimental arrangement to test the QCD energy-energy cross section was given in our previous letter (Ref. 15). This entailed measurements at $\theta = 90^\circ$ with unpolarized beams involving the quantity

$$\begin{aligned} A(\xi) &= \frac{16\pi^3}{\bar{g}(W)^2} [\mathcal{A}(\chi)(1 + \xi - \xi^2) \\ &+ \mathcal{A}(\chi)\left(\frac{1}{2} - \xi\right)] \end{aligned}$$

and the difference

$$\begin{aligned} D_A(\xi) &= A(1 - \xi) - A(\xi) \\ &= \frac{16\pi^3}{\bar{g}(W)^2} \{ \mathcal{D}(\chi)(1 + \xi - \xi^2) \\ &\quad - [\mathcal{B}(\chi) + \mathcal{B}(\pi - \chi)]\left(\frac{1}{2} - \xi\right) \}. \end{aligned}$$

¹⁸G. 't Hooft and M. Veltman, *Nucl. Phys.* **B44**, 189 (1972); C. G. Bollini and J. J. Giambiagi, *Nuovo Cimento* **12B**, 20 (1972); J. F. Ashmore, *Lett. Nuovo Cimento* **4**, 289 (1972); R. Gastmans and R. Meuldermans, *Nucl. Phys.* **B63**, 277 (1973); R. Gastmans, J. Verwaest, and R. Meuldermans, *ibid.* **B105**, 454 (1976). For a review see G. Liebrandt, *Rev. Mod. Phys.* **47**, 849 (1975). The work closest to ours is that of W. J. Marciano, *Phys. Rev. D* **12**, 3861 (1975), who employs dimensional continuation as a means of regulating infrared divergences in real processes for

theories with massless particles.

¹⁹The convention employed here differs from that of our previous work (Ref. 9) in that the density matrix for the virtual photon spin is now normalized to have a unit trace.

²⁰See, for example, *Higher Transcendental Functions*,

(Bateman Manuscript Project), edited by A. Erdélyi (McGraw-Hill, New York, 1953), Vol. I, Chap. II.

²¹Our calculation for the vertex differs somewhat from that of W. J. Marciano cited in Ref. 18 in that we use Feynman rather than Landau gauge.

²²See, e.g., L. S. Brown, Phys. Rev. D 5, 748 (1972).